AD-A070 742 MARTIN MARIETTA LABS BALTIMORE MD F/G 20/4
UNSTEADY BOUNDARY LAYER SEPARATION.(U)
APR 79 K C WANG N00014-77-C-0650
UNCLASSIFIED MML-TR 79-16C NL

1 OF 1
AD A070 742

END
DATE FILMED
8-79
DDC

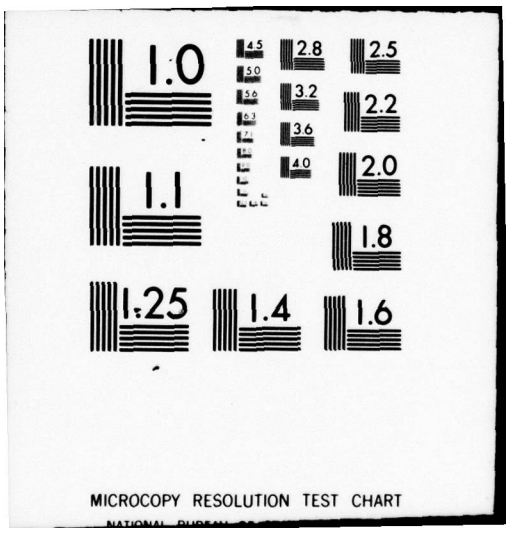
1.0
1.1
1.25
1.4
1.6
1.8
2.0
2.2
2.5
2.8
3.2
3.6
4.0
4.5
5.0
5.6
6.3
7.1
MICROCOPY RESOLUTION TEST CHART

LEVEL II

MML TR 79-16c

UNSTEADY BOUNDARY LAYER SEPARATION

K. C. Wang

April 1979

Research sponsored by the U.S. Office of Naval Research under Contract N00014-77-C-0650

UNSTEADY BOUNDARY LAYER SEPARATION

K. C. Wang

MML TR 79-16c

April 1979

Research Sponsored by the Office of Naval Research,
United States Navy, under Contract N00014-77-C-0650

Martin Marietta Corporation
Martin Marietta Laboratories
1450 South Rolling Road
Baltimore, Maryland 21227

SECURITY CLASSIFICATION OF THIS PAGE (When Data Entered)

REPORT DOCUMENTATION PAGE

READ INSTRUCTIONS BEFORE COMPLETING FORM

1. REPORT NUMBER: MML TR 79-16c
2. GOVT ACCESSION NO.:
3. RECIPIENT'S CATALOG NUMBER:
4. TITLE (and Subtitle): Unsteady Boundary Layer Separation
5. TYPE OF REPORT & PERIOD COVERED: Technical Report
6. PERFORMING ORG. REPORT NUMBER: MML-TR 79-16c
7. AUTHOR(s): K. C. Wang
8. CONTRACT OR GRANT NUMBER(s): N00014-77-C-0650
9. PERFORMING ORGANIZATION NAME AND ADDRESS:
Martin Marietta Laboratories
Martin Marietta Corporation
1450 South Rolling Road, Baltimore, Maryland 21227
10. PROGRAM ELEMENT, PROJECT, TASK AREA & WORK UNIT NUMBERS:
11. CONTROLLING OFFICE NAME AND ADDRESS:
Office of Naval Research
Code 438
Arlington, Virginia 22217
12. REPORT DATE: April 1979
13. NUMBER OF PAGES: 57
14. MONITORING AGENCY NAME & ADDRESS (if different from Controlling Office):
15. SECURITY CLASS. (of this report): Unclassified
15a. DECLASSIFICATION/DOWNGRADING SCHEDULE:

16. DISTRIBUTION STATEMENT (of this Report)

Approved for public release; distribution unlimited.

17. DISTRIBUTION STATEMENT (of the abstract entered in Block 20, if different from Report)

18. SUPPLEMENTARY NOTES

19. KEY WORDS (Continue on reverse side if necessary and identify by block number)

Unsteady separation in 2 and 3 dimensions
Separation criteria
Unsteady boundary layers
Numerical solutions

20. ABSTRACT (Continue on reverse side if necessary and identify by block number)

A new separation criterion for two-dimensional unsteady boundary layers is proposed here. This criterion is derived by analogy, from its counterpart for steady, three-dimensional boundary layers. Analogous limiting streamlines for the unsteady, two-dimensional case are first defined, and an envelope of these streamlines is used to signify unsteady separation. To demonstrate this procedure, two previously studied problems are recalculated here. These are the unsteady responses to (1) a sudden change in velocity in Howarth's problem, and (2) an impulsively-started circular cylinder. Our conclusion regarding

(contd reverse side)

DD FORM 1 JAN 73 1473 EDITION OF 1 NOV 65 IS OBSOLETE

407 998

SECURITY CLASSIFICATION OF THIS PAGE (When Data Entered)

(20) contd
separation for the cylinder problem disagrees with that of Telionis and Tsahalis based on the singularity criterion, but appears to be consistent with the prediction of Proudman and Johnson. Finally, we propose a three-dimensional, unsteady separation criterion on the basis of repeated applications of either the steady, three-dimensional separation criterion at successive times or the unsteady, two-dimensional separation criterion at fixed coordinate planes.

CONTENTS

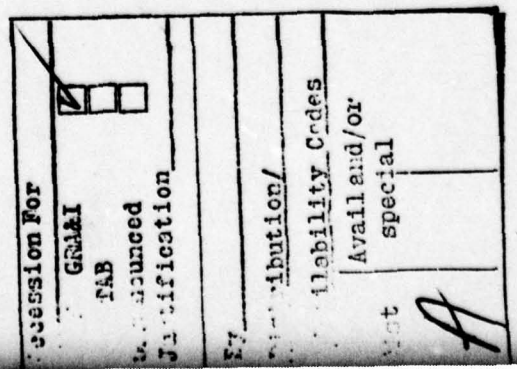

SUMMARY

A new separation criterion for two-dimensional unsteady boundary layers is proposed here. This criterion is derived by analogy, from its counterpart for steady, three-dimensional boundary layers. Analogous limiting streamlines for the unsteady, two-dimensional case are first defined, and an envelope of these streamlines is used to signify unsteady separation. To demonstrate this procedure, two previously studied problems are recalculated here. These are the unsteady responses to (1) a sudden change in velocity in Howarth's problem, and (2) an impulsively-started circular cylinder. Our conclusion regarding separation for the cylinder problem disagrees with that of Telionis and Tsahalis based on the singularity criterion, but appears to be consistent with the prediction of Proudman and Johnson. Finally, we propose a three-dimensional, unsteady separation criterion on the basis of repeated applications of either the steady, three-dimensional separation criterion at successive times or the unsteady, two-dimensional separation criterion at fixed coordinate planes.

1. UNSTEADY SEPARATION IN TWO DIMENSIONS

1.1. Introduction

For steady, two-dimensional boundary layers, the separation criterion first conceived by Prandtl is defined by the vanishing of skin friction. This definition is mathematically simple and precise, and its application is convenient. Associated with this idea of separation, there have also been a number of common notions or symptoms, each of which characterizes a certain aspect of the whole phenomenon. These include:

1. Singularity - separation is said to reflect mathematically a singularity of the boundary layer solution.
2. Reverse flow - separation is said to signify the onset of flow reversal.
3. Inaccessibility - separation determines a separated region which is inaccessible to the upstream flow.
4. Boundary layer thickening - separation is marked by a rapid growth of the boundary layer thickness.
5. Breakdown of boundary layer assumptions - separation means that the basic boundary layer assumptions become invalid.
6. Computation difficulties - convergence difficulty and increase of the number of iterations imply separation.

Some of these factors, individually or in combination, have become synonymous with separation and have even been taken as alternative definitions. Indeed, it is interesting to note that these charactristics almost imply one another in two-dimensional steady flow.

In the present study, however, we were concerned to know whether these ideas are valid for the two-dimensional, unsteady case. We concluded that some of these are valid while some are not, and that new ones are needed.

Items 4 thru 6, for example, are by and large still valid, but are not suitable separation criteria. The breakdown of boundary layer assumptions is only a general qualitative statement, not a quantitative, implementable criterion. The rapid growth of boundary layer thickness and the computational difficulties are imprecise and unreliable, and computational difficulties can be caused for reasons other than separation.

Rott (1956) first pointed out that zero skin-friction does not necessarily mean separation for moving walls. Moore (1958) recognized the same, and proposed what is now known as the MRS (after Moore, Rott and Sears) criterion. A similar conclusion was also reached by Stewartson (1960), who went on to distinguish between the term "separation" and "breakdown," or "breakaway." "Separation" is made to refer to the zero-skin-friction point at the body, while "breakdown" is used to signify other symptoms usually related to separation. Further investigations on unsteady separation were undertaken more recently by Sears and Telionis (1971, 1975), who attempted to generalize mathematically the validity of the Goldstein singularity and the MRS criterion for general unsteady boundary layers. Telionis and Tsahalis (1974a, b) presented calculated examples in support of the Goldstein singularity criterion, while Williams and Johnson (1974a, b) did the same for the MRS criterion. As more will be discussed later, items 1 through 3 no longer hold for the unsteady case.

In this work, we shall first briefly review the work of Moore, and of Sears and Telionis (Section 1) and then propose a new unsteady separation criterion (Section 2) based on an analogy to the envelope criterion for the steady, three-dimensional case. Next, calculated examples are presented in Section 3. Finally, the envelope criterion for the steady, three-dimensional case is applied at successive instants of time in order to derive a three-dimensional unsteady separation criterion. The same objective can be realized by applying repeatedly the just-mentioned two-dimensional unsteady separation criterion. Thus, the resulting unsteady, three-dimensional separation criterion may be looked upon as a unified separation criterion including as special cases those for two-dimensional, unsteady separation and three-dimensional, steady separation.

A word of caution is needed regarding the coordinate notations. In Section 1, because we shall for the most part review the literature on the subject, it is desirable to retain the usual convention of denoting the coordinates parallel and normal to the body, x and y, where u is the velocity along the x-direction. In subsequent sections, z is used to denote the normal direction in accordance with the convention for three-dimensional space, while other changes are introduced as they may arise. Time is designated "t" throughout this work.

1.2. MRS Criterion and Goldstein Singularity

In a classical paper on unsteady separation, Moore (1958) defined the separation for a steady moving-wall problem by

$$\left.\begin{aligned} u &= 0 \\ \frac{\partial u}{\partial y} &= 0 \end{aligned}\right\} \text{ at } y > 0. \qquad (1a,b)$$

Here separation is marked by the simultaneous vanishing of velocity and shear at some point above the wall. In contrast, these two conditions are satisfied at a fixed wall for the usual two-dimensional steady case. Moore illustrated the flow patterns as well as the velocity profiles as shown in figure 1.

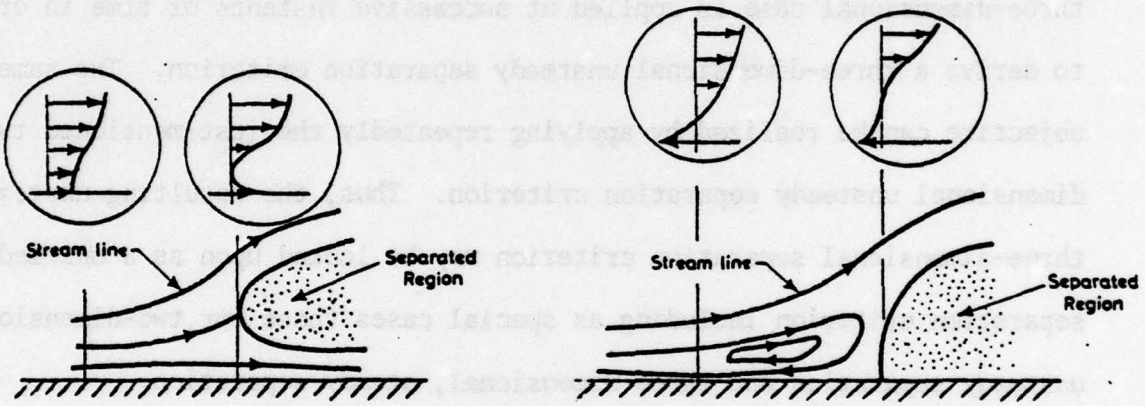

Figure 1. MRS separation model for a moving wall. (a) wall moving downstream, (b) wall moving upstream.

Moore also suggested that equations (1a,b) may be applied to a quasi-steady boundary layer in a coordinate moving with the separation point, and that Goldstein's (1948, Stewartson 1958) singularity for a steady flow may also exist in the unsteady case.

Sears and Telionis (1971, 1975) pursued further the unsteady separation question and attempted to generalize mathematically the validity of Goldstein's singularity and the MRS criteria for general unsteady boundary layers. Following Landau's (1959) approach to the Goldstein singularity problem, Sears and Telionis expanded near the center of separation $(x_o y_o)$ (Figure 2).

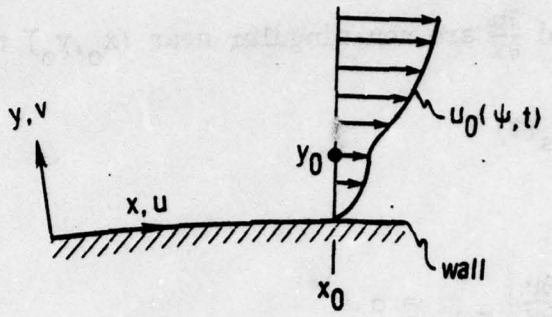

Figure 2. Goldstein's singularity.

$$u(x,y,t) = u_o(\psi,t) + \frac{\partial\beta(\psi,t)}{\partial y}\sqrt{x_o - x} + \frac{\partial\beta_1(\psi,t)}{\partial y}(x_o - x) + \ldots, \quad (2)$$

$$v(x,y,t) = \frac{\beta(\psi,t)}{2\sqrt{x_o - x}} + \beta_1(\psi,t) + \ldots, \quad (3)$$

where

$$\psi = y - y_o(t), \quad (4)$$

$$u_o(\psi,t) = u(x_o,y,t). \quad (5)$$

Except that y_o, u_o, β, and β_1 are allowed to be time dependent here, these expansions are otherwise identical to Landau's. Sears and Telionis identified

$$\beta(\psi,t) = A(t)\ [u_o(\psi,t) - U_s(t)], \quad (6)$$

where $A(t)$, $u_o(\psi,t)$ remain undetermined and

$$U_s(t) = \frac{dx_o}{dt}, \quad (7)$$

i.e., U_s is defined as the velocity of the center of separation. By

insisting that v and $\frac{\partial u}{\partial x}$ are non-singular near (x_o, y_o) they obtained

$$u_o(\psi=0,t) = U_s(t) \,, \tag{8}$$

and

$$\frac{\partial u_o(o,t)}{\partial y} = \left.\frac{\partial u}{\partial y}\right|_{y=y_o} = o \,. \tag{9}$$

Equation (8) states that the center of separation is a moving stagnation point, and equation (9) says that the shear vanishes at (x_o, y_o). Thus equations (2) through (7) are considered to describe an analysis of the unsteady Goldstein singularity, and equations (8), (9) to establish the MRS criterion for general unsteady boundary layers.

The preceding analysis is not free from uncertainty. First, it is obviously incomplete and hence not very convincing to say that the Goldstein singularity or the MRS criterion has been demonstrated for a general unsteady case. Second, the assumption that v and $\frac{\partial u}{\partial x}$ are non-singular near (x_o, y_o) -- the basis for equations (8) and (9) -- seems to be arbitrary and no justification has been given, except that it leads immediately to the desired conclusions. This assumption does not appear to be consistent with its converse; i.e., v and $\frac{\partial u}{\partial x}$ are singular at $x = x_o$, the basis for the expansion of equations (2) and (3), unless one argues that v and $\frac{\partial u}{\partial x}$ are singular along the line $x = x_o$, excluding the particular point (x_o, y_o) and its neighborhood in the middle.

The concept of MRS criterion certainly has an intuitive appeal in a steady moving-wall problem, and its validity there can be readily accepted. It is also clear that such steady flow over a moving-wall becomes unsteady to an observer fixed with the wall or the separation point. However, it

remains to be demonstrated that general unsteady boundary layers can be looked upon in the same light and that general unsteady separation is determined by the same MRS criterion in a coordinate system moving with separation. Although solutions due to Williams and Johnson (1974a,b) and Williams (1977) provided support to the MRS criterion, their special assumptions regarding the relation between x and t virtually reduce unsteady problems to steady ones for which, as noted above, there is little doubt respecting its validity.

Later papers by Telionis and Tsahalis (1974a,b) presented calculated results, mostly for the normal velocity, and these were interpreted to exhibit the features of Goldstein singularity. However, a recent calculation of Cebeci (1978) has contradicted their claims in the circular cylinder problem; and similar disagreements are also noted in this work (Section 3.3).

Aside from considerations of validity, neither the MRS criterion nor the Goldstein singularity criterion is convenient to apply. In the case of the MRS criterion, there is the need to define a coordinate system moving with the velocity at separation which, in turn, is not known until the location of separation is determined. Thus, iteration is necessary. In the case of the singularity criterion also there is no simple way to know where the Goldstein singularity is located. For numerical solutions, the separation is still decided by the usual symptoms such as rapid change of the normal component of velocity, boundary layer thicknesses, skin friction, or the increase of the number of iterations, etc., while the criterion will be used only afterwards to help interpret the results.

However, deciding whether particular results really exhibit typical square-root singularity can be rather uncertain.

Both the unsteady MRS criterion and the unsteady Goldstein singularity were extended from their counterparts for conventional, two-dimensional, steady flows. Their extension to three-dimensional case remains to be demonstrated. In contrast, the unsteady, two-dimensional envelope criterion proposed in Section 2 or the analogous three-dimensional steady separation criterion can be readily generalized to yield a three-dimensional, unsteady separation criterion (see Section 4).

2. ANALOGY APPROACH AND THE PROPOSED SEPARATION CRITERION

2.1 Unsteady Analogy

The analogy approach for the two-dimensional unsteady boundary layer is based on the observation that the relevant system of governing equations embodies a mathematical structure similar to that for the steady, three-dimensional boundary layer. The latter problem has been extensively investigated in recent years by the author (Wang 1970, 1972, 1974, 1975a, 1976), and results have revealed new features of fundamental significance. By analogy, what has been learned from these investigations can be applied to the two-dimensional, unsteady case. Various aspects of such an analogy were also previously noted by a number of authors, including Stewartson (1960, 1963), Hall (1968), Dwyer (1969), Krause etc. (1969) and Patel and Nash (1971, 1976).

Based on the unsteady analogy, Wang (1975b) extended the concept of the zone of dependence and influence for the steady, three-dimensional case (Wang, 1971) to the unsteady, two-dimensional case. The dependence rule is especially important with respect to the finite-difference method of solution because it serves as a criterion for determining the convergence and stability of numerical solutions. Wang (1975b) further pointed out (1) that the reversal of the crossflow over an inclined body (a typical, steady three-dimensional problem) can be calculated as long as the dependence is satisfied, and that (2) neither the vanishing of skin friction nor the reversal of the crossflow necessarily signifies

separation. By analogy, reversed flow in the two-dimensional unsteady case can also be calculated after passing through the zero skin-friction point so long as the corresponding dependence rule is satisfied. These conclusions agree both with the MRS criterion regarding that the vanishing of skin friction does not mean separation, and with the work of Telionis and Tsahalis (1974a,b) and Phillips and Ackerberg (1973) regarding the calculability of unsteady reversed flow; however, our conclusions were reached from a different viewpoint. In the present investigation we applied the unsteady analogy to the question of separation.

2.2. Formal Reduction of Equations

We could start from the most general, steady, three-dimensional boundary layer equations to demonstrate their reduction to those for the two-dimensional, unsteady case. However, since we planned to employ our existing computing codes originally developed for the steady, three-dimensional case to calculate examples for the present two-dimensional, unsteady case (Section 3), we chose to start from the equations written for a body of revolution (figure 3). However, this imposes no restriction

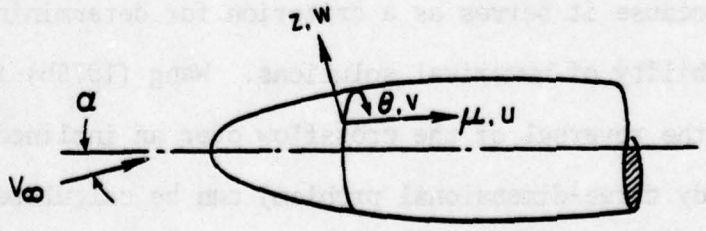

Figure 3. Flow over an ellipsoid of revolution.

on the analogy discussed here, because, as we shall point out, the same set of unsteady equations will result by the virtue of the analogy transformation, equation 16.

The coordinate system (figure 3) consists of μ, θ, z, where μ and θ are parallel to the body surface and z is normal to the body surface; h_μ, h_θ are the corresponding metric coefficients; and u, v, w are the velocities. Reversal of the v-velocity is allowed in our computing codes. The relevant equations are:

$$u\frac{\partial u}{h_\mu \partial \mu} + v\frac{\partial u}{h_\theta \partial \theta} + w\frac{\partial u}{\partial z} - v^2\frac{\partial h_\theta}{h_\mu h_\theta \partial \mu} = \frac{-\partial p}{h_\mu \partial \mu} + \frac{\partial^2 u}{\partial z^2}\,, \tag{10a}$$

$$u\frac{\partial v}{h_\mu \partial \mu} + v\frac{\partial v}{h_\theta \partial \theta} + w\frac{\partial v}{\partial z} + uv\frac{\partial h_\theta}{h_\mu h_\theta \partial \mu} = \frac{-\partial p}{h_\theta \partial \theta} + \frac{\partial^2 v}{\partial z^2}\,, \tag{10b}$$

$$\frac{\partial u}{h_\mu \partial \mu} + u\frac{\partial h_\theta}{h_\mu h_\theta \partial \mu} + \frac{\partial v}{h_\theta \partial \theta} + \frac{\partial w}{\partial z} = 0, \tag{10c}$$

with the boundary conditions:

$$u = v = w = 0 \quad \text{at } z \to 0\,, \tag{11a}$$

$$u = U, \quad v = V, \text{ at } z \to \infty,$$

where U and V are the corresponding outer-edge velocities.

The pressure relations are given by

$$\frac{-\partial p}{h_\mu \partial \mu} = U\frac{\partial U}{h_\mu \partial \mu} + V\frac{\partial U}{h_\theta \partial \theta} - V^2\frac{\partial h_\theta}{h_\mu h_\theta \partial \mu}\,, \tag{12a}$$

$$\frac{-\partial p}{h_\theta \partial \theta} = U\frac{\partial V}{h_\mu \partial \mu} + V\frac{\partial V}{h_\theta \partial \theta} + UV\frac{\partial h_\theta}{h_\mu h_\theta \partial \mu}\,. \tag{12b}$$

The limiting streamlines are defined by

$$\frac{h_\theta d\theta}{h_\mu d\mu} = \frac{(v)_{z=o} + \left(\frac{\partial v}{\partial z}\right)_{z=o} \Delta z + \cdots}{(u)_{z=o} + \left(\frac{\partial u}{\partial z}\right)_{z\to o} \Delta z + \cdots} \cong \frac{c_{f\theta}}{c_{f\mu}}, \tag{13}$$

where $c_{f\theta}$ and $c_{f\mu}$ are the skin-friction coefficients along the θ- and μ- directions. They are defined by

$$\sqrt{R}\, c_{f\theta} = \left(\frac{\partial v}{\partial z}\right) z\to o, \tag{14a}$$

$$\sqrt{R}\, c_{f\mu} = \left(\frac{\partial u}{\partial z}\right) z\to o, \tag{14b}$$

where R is the Reynolds number.

The two components of displacement thickness are

$$\Delta_\theta = \frac{V}{\sqrt{U^2+V^2}} \int_o^\infty (1-v/V)dz, \tag{15a}$$

$$\Delta_\mu = \frac{U}{\sqrt{U^2+V^2}} \int_o^\infty (1-u/U)dz \quad . \tag{15b}$$

To obtain the formal unsteady analogy, we let

$$\begin{aligned} \mu &\to t, & u &\to 1, \\ \theta &\to x, & U &\to 1, \\ z &\to z, & h_\mu &\to 1, \\ & & h_\theta &\to h_x(x). \end{aligned} \tag{16}$$

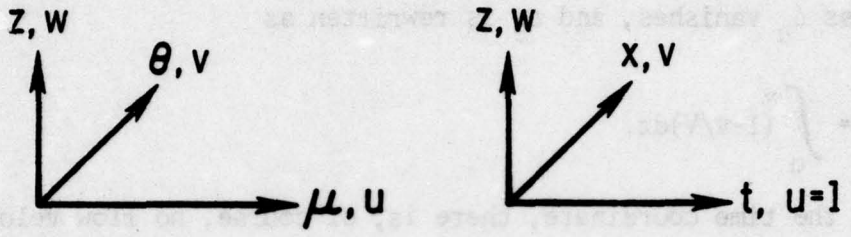

Figure 4. Coordinate transformation.

Then equation 10(a) vanishes identically, and equations 10(b,c) become

$$\frac{\partial v}{\partial t} + v\frac{\partial v}{h_x \partial x} + w\frac{\partial v}{\partial z} = -\frac{\partial p}{h_x \partial x} + \frac{\partial^2 v}{\partial z^2}, \tag{17a}$$

$$\frac{\partial v}{h_x \partial x} + \frac{\partial w}{\partial z} = 0. \tag{17b}$$

The boundary conditions (11a,b) become

$$v = w = o \quad \text{at } z = o, \tag{18a}$$

$$v = V \quad \text{at } z \to \infty. \tag{18b}$$

The pressure relation (12a) vanishes, equation 12(b) becomes

$$-\frac{\partial p}{h_x \partial x} = \frac{\partial V}{\partial t} + V\frac{\partial V}{h_x \partial x}. \tag{19}$$

The limiting streamline equation (13) is reduced to

$$\frac{h_x dx}{dt} = \left(\frac{\partial v}{\partial z}\right)_{z=o} \Delta z, \tag{20}$$

$$= \sqrt{R}\, c_f \Delta z,$$

where the definition of skin-friction c_f follows from equation 14(a,b), $c_{f\theta}$ is redesignated as c_f, and $c_{f\mu}$ vanishes. Similarly the displacement thickness Δ_μ vanishes, and Δ_θ is rewritten as

$$\Delta = \int_o^\infty (1-v/V)dz. \tag{21}$$

In the time coordinate, there is, of course, no flow velocity to speak of. Formal analogy is achieved by imposing u = 1 throughout the whole flow field. A uniform flow component along a particular dimension does not affect the rest of flow and, hence, is effectively the same as no flow component at all along that direction. Also noteworthy is that the condition u = 1 is applied even at z = o, although this seems to be incompatible with the no-slip condition in equation 11(a). However, our rationalization here is that the uniform flow is only an imaginary one to achieve formal analogy, and, hence, relaxing the no-slip condition is of no consequence. On the other hand, insistence on a no-slip condition would have introduced a vortex sheet at the wall, making uniform flow as conceived impossible.

Next, equations 10 and 12 differ from those for the most general three-dimensional boundary layer equations only in terms containing $\partial h_\mu/\partial\theta$. Since h_μ is taken to be 1 in the analogy transformation, those terms would have disappeared anyway. Hence our use of equations 10(a,b,c) as the starting point of discussion causes no loss of generality.

It is noteworthy that implicit in the no-slip condition (18a), v = o at z = o, the coordinate system is fixed with the body. Also among the preceding reductions of equations, the reduction from equation (13) to

equation (20) is of particular interest in the present work because it continues the concept of the limiting streamlines for which the pattern forms the basis of determining separation.

Equations 17 through 21 are all written in nondimensional forms: t is non-dimensionalized with a/V_∞; a is a typical length, V_∞ the velocity at infinite; x is non-dimensionalized with a, v with V_∞, z with $a/\sqrt{R}$, w with $V_\infty/\sqrt{R}$, p with $\rho_\infty V_\infty^2$ where $R(=Va/\nu)$ is the Reynolds number, ν the kinematic viscosity, ρ_∞ the density at infinite. All these variables are thus in the physical forms, and no transformed variable is used.

2.3 Proposed Unsteady Separation Criterion

2.3.1. Steady, three-dimensional separation

Separation of steady, three-dimensional flows has been discussed recently by Wang (1976) in some length. Here only a brief recapitulation is given to provide a background for introducing our proposed unsteady separation criterion.

For steady, three-dimensional flows, the separation line on a body surface can be readily identified from a surface-flow visualization experiment. In such flow photographs, the limiting streamlines are made clearly visible. As these limiting streamlines approach a separation line, they turn tangentially to merge with the latter. The separation line obtained in this way has the appearance of an envelope for the limiting streamlines (figure 5). In recent years, numerical solutions of full three-dimensional boundary layer equations have actually calculated the limiting streamlines according to equation (13), and the formation of an envelope has been theoretically confirmed (for example, Wang, 1974, 1975a).

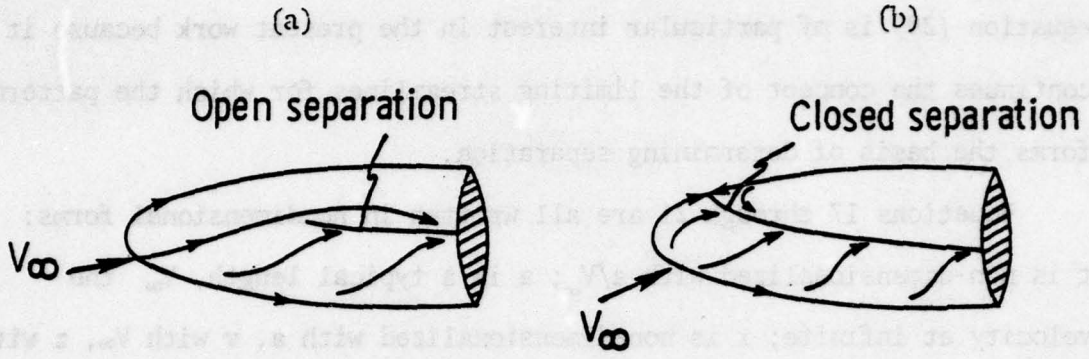

Figure 5. Three-dimensional, steady separation.
(a) Open separation.
(b) Closed separation.

Separation on a body surface can be classified into an open type (figure 5a) and a closed type (figure 5b). Conventional concepts of three-dimensional separation fall into the closed type. An open separation is a new concept (Wang 1972, 1974, 1976). By an open separation is meant that the separation line is not closed in the front leeside surface and does not originate or terminate at singular points in the sense that both skin-friction components vanish. The limiting streamlines on both sides of the separation line originate from the same front attachment point; i.e., the separated region is accessible to upstream flow. In contrast, for a closed separation, the separation line is closed around the body, passing through the singular points of the limiting streamlines so that the limiting streamlines on two sides of the separation line originate from two different attachment points.

There is no surface flow across separation line, open or closed (similarly for the separation surface above the wall). In other words, the skin-friction component normal to the separation line vanishes. Along

the separation line, the limiting flow is therefore confined to the plane normal to the body, and tends to lift-off as the word "separation" implies.

It may be asked at this point why the vanishing of normal skin friction cannot be taken as a definition of separation analogous to Prandtl's zero-wall-shear criterion for two-dimensional flows. The answer is that actual determination of separation in accordance with this definition (i.e. vanishing of normal skin friction) is rather difficult, if not impossible, because the separation line and its normal direction are not known a priori. The vanishing of normal skin friction seems to be more a consequence or symptom of the separation phenomenon, instead of a conveniently implementable criterion. Its relation to Prandtl's zero-wall-shear criterion is also shallow because the simplicity, convenience and some of the immediate consequences of Prandtl's criterion are missing.

2.3.2. Usteady two-dimensional separation

In analogy with equation 13, equation 20

$$\frac{h_x dx}{dt} = \left(\frac{\partial v}{\partial z}\right)_{z \to o} \Delta z \ ,$$

may determine a family of limiting streamlines in the x,t-plane for the unsteady, two-dimensional case, and these streamlines may also form an envelope (figure 6). The skin friction $\sqrt{R}\, c_f = \left(\frac{\partial v}{\partial z}\right)_{z \to o}$ as a function of x,t must be first obtained from the complete boundary layer equations 17(a) and (b). Δz is taken as a constant whose actual value has the same effects as the length scales in an x,t-diagram, but it does not change the physics of the problem. For convenience, Δz may be set equal to 1.

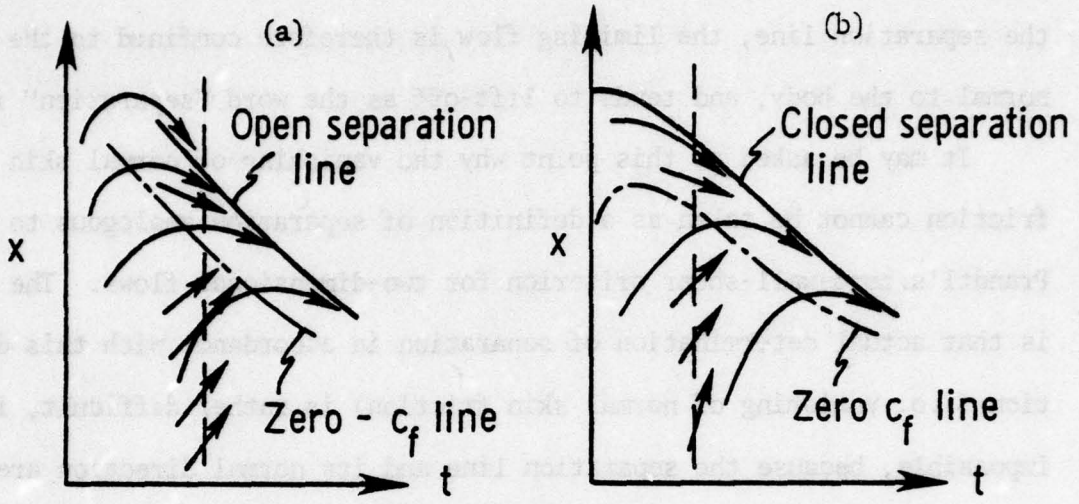

Figure 6. Two-dimensional unsteady separation.
(a) Open separation.
(b) Closed separation.

At each point (x,t), an arrow is drawn based on the skin-friction value to represent the local direction so that the lines drawn parallel to these arrows represents the analogous limiting streamlines. As these lines cross the zero-skin-friction line, they turn downward, posing a question as to whether an envelope to these limiting streamlines will be formed.

It is the author's contention that such an envelope in the x,t-plane may be taken as an indication of unsteady separation. Furthermore, unsteady, two-dimensional separation may also be classified into an open type (figure 6a) and a closed type (figure 6b). An unsteady open separation means that the separation line does not divide the x,t-plane into two unconnected regions. Therefore, it can be approached on both sides by limiting streamlines originating from the front body at earlier times. Separation does not occur at every instant of time. The unsteady growth

of an impulsively-started motion from rest provides an example of open separation, because at early times, the flow is inviscid and there is no separation to speak of. Separation occurs only over the rear side at large times. In contrast, an unsteady closed type of separation means that separation occurs at every instant of time, and the separation line divides the x,t-plane into two unconnected regions approached on two sides by limiting streamlines not originating from the same side in the x,t-plane.

According to the MRS criterion, unsteady separation can no longer be characterized by the wall shear. Instead, it must be determined by the shear somewhere above the wall. While we agree that the zero-skin-friction does not imply unsteady separation, it does not follow that unsteady separation can not be characterized by the skin friction. It appears to us that the question really hinges on what information about the skin friction one chooses to use, the vanishing of local c_f or the limiting streamline pattern. In our study, we chose the streamline pattern to determine separation; and this streamline pattern depends, in turn, on the skin friction distribution $c_f(x,t)$ as a function of x and t.

The right hand side of equation 20, $\left(\frac{\partial v}{\partial z}\right)_{z \to o} \Delta z$, represents a limiting velocity. At first glance, it may be thought that equation 20 determines a path line, but this is not so because the limiting velocity is determined by Eulerian formulation rather than by following a particular fluid particle. Equation 20 actually defines lines the direction of which in the x,t-plane coincides with the limiting velocity ($z \to o$) at that particular time and space. In this sense, they are more appropriately called streamlines. However, since t is not a space coordinate, they are not the streamlines as usually understood.

3. CALCULATED EXAMPLES

To demonstrate the proposed separation criterion, two problems previously studied by Telionis and Tsahalis (1974a,b) are reconsidered here. The first is concerned with the unsteady response to an impulsive change of Howarth's linear outer-flow; the second deals with the boundary layer growth over a circular cylinder impulsively started from rest. In either case, the sudden change of the outer velocity immediately generates a vortex sheet on the body due to the no-slip boundary condition. The subsequent diffusion of such a vortex sheet in addition to convective flow is the central physical process in these problems, which are intended to demonstrate respectively closed and open separations.

3.1. Method of Calculation

Our computing programs previously developed for the steady, three-dimensional boundary layers were modified for the present unsteady calculations, and two finite-difference schemes (Wang 1975b) were used. For a fixed time t, scheme "a" (figure 7a) is first called for the non-reversed flow region; then scheme "b" (figure 7b) is called for the reversed flow

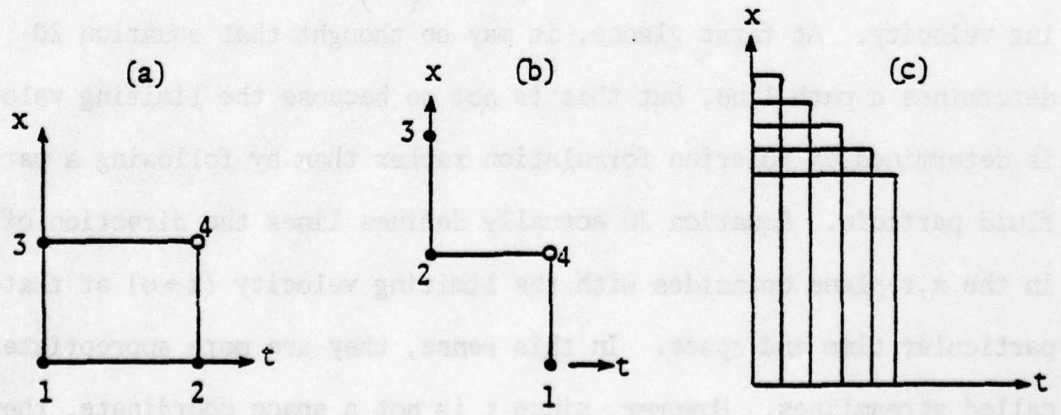

Figure 7. Computation meshes.
(a) Scheme a. (b) Scheme b.
(c) Loss of points as t advances.

region. In either scheme, point 4 is the unknown point to be determined from known points 1, 2, 3, and the unsteady rule of dependence zone is fulfilled at every point (x,t). Because of lack of initial data, employment of the zig-zag scheme (figure 7b) necessitates, in general, the loss of one x-station for each t-constant line (figure 7c). This means that small Δx and large Δt must be used. Otherwise the calculable range in both the x- and t-direction would be significantly curtailed and less reversed flow would be determined.

Actually scheme "b" is applicable to both reversed and non-reversed flow regions, but scheme "a" has the advantages of simplicity while not losing a space station as in scheme "b" when no reversed flow is involved in a whole t-constant line. Hence, if these two schemes are used in combination, the range of calculation can be extended beyond what would be the case if scheme "b" alone were used throughout the whole calculation. Computation proceeds first along the space coordinate from the leading-edge or the front stagnation point downstream, then advances in time.

3.2 Impulsive Change of Howarth's Problem

To study steady separation, Howarth (1938) considered the boundary layer with an outer velocity $V = 1-ax$ where a is a constant. Our present objective is to study the unsteady response of such a boundary layer when V suddenly changes from V_1 to V_2 (Telionis and Tsahalis, 1974a) where

$$V_1 = 1-a_1x, \tag{22a}$$

$$V_2 = 1-a_2x\ . \tag{22b}$$

a_2 shall be chosen to be greater than a_1 so that the separation point corresponding to V_2 will be upstream of the separation point corresponding to V_1. This is due to the fact that the current initial-value finite-difference method of solution can only handle the case when separation moves upstream.

Furthermore, when $\Delta V = V_2 - V_1$ is small compared to V_1 and V_2 (i.e., small change), the boundary layer response will be slow in reaching the final steady-state. This consideration tends to suggest that the present problem may not be a suitable example for studying unsteady boundary layer growth even though simple linear outflow served well for Howarth's original purpose. However, in order to demonstrate our proposed separation criterion, this consideration is only a side issue.

To start numerical solutions, the temporal initial profiles $v(x,z,t_o)$ and the spatial initial profiles $v(x_o,z,t)$ are needed. The temporal initial profiles may be obtained from the first approximation of the usual small-time expansion (see Schlichting 1968, Telionis and Tsahalis 1974a), i.e.,

$$v(x,z,t_o) = v_{H1}(x,z) + (V_2-V_1)\mathrm{erf}\left(\frac{z}{2\sqrt{t_o}}\right) \quad , \tag{23}$$

where the first term represents Howarth's steady solution coresponding to V_1, which prevails for $t \leq o$, and the second term represents viscous diffusion due to the sudden changes V_2-V_1, with erf as the error function.

The spatial initial profiles may be obtained from the steady solution for either V_1 or V_2 valid at small x. This is because diffusion and convection affect the downstream flow only; consequently, solution near $x = o$ is nearly independent of time. Furthermore, for small x, V_1 and V_2 are

almost equal. The required initial profiles may be taken either from the numerical solution of the steady problem at small x or from Howarth's series solution with the first term only (Howarth 1938).

Since Howarth's series solution is believed not to be accurate enough for large x, the required Howarth's steady-state solutions corresponding to V_1 and V_2 were first obtained by a separate computing program. In doing this, it was found that results are very sensitive to the edge-condition, i.e.,

$$\left(\frac{\partial v}{\partial z}\right)_{z=\infty} = 0 \quad \text{or} \quad \frac{V-v_{N-1}}{V} < \varepsilon \ , \tag{24}$$

where V_{n-1} is the velocity just one Δz below the outer edge. Although $\varepsilon = 0.01$ is normally considered to be reasonable, it gives unacceptable results for the present problem. The skin friction distributions with $\varepsilon = 0.005$ and 0.0025 for A = 0.05 and 0.07 are shown in figure 8, and they still reveal some differences. The separation point is located at x = 1.78 and 2.42 for $\varepsilon = 0.0025$, and at 1.81 and 2.52 for $\varepsilon = 0.005$. These values are a little higher than those given by Howarth, and by Telionis and Tsahalis whose values are 1.71 and 2.40.

By setting $h_x = 1$, equations 17 and 18 can now be calculated with those known initial profiles. The initial time and space were chosen as $t_o = 0.06$ and $x_o = 0.0134$. The range of calculation extends spacewise $0.134 \leq x \leq 2.5$ and timewise $0.06 \leq t \leq 38$. The x step, Δx, was 0.005, and several values of the time step $\Delta t = 0.04, 0.10, 0.25, 0.50$ were used. Smaller values (0.04, 0.10) were used at early times ($t \leq 1.0$); larger ones (0.25, 0.50) were used at later times, a value of 0.25 was used for $1.0 \leq t \leq 13$ and 0.5 for the rest.

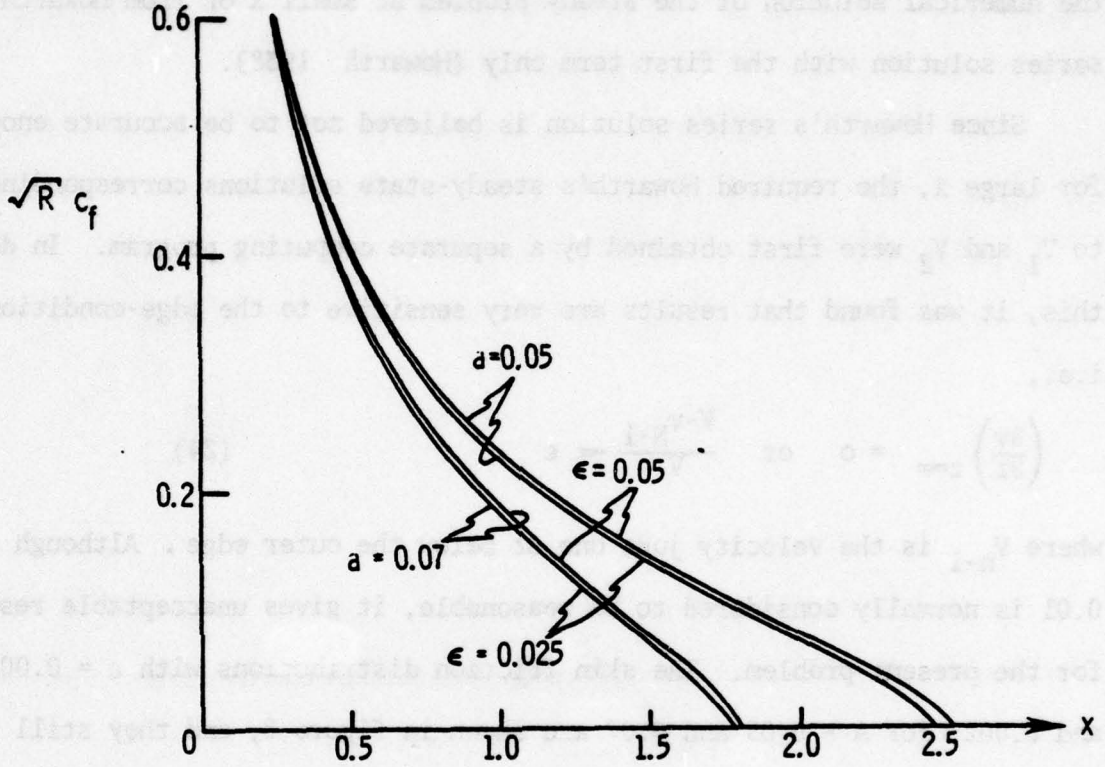

Figure 8. c_f of Howarth's steady-state problem.

The calculated skin friction c_f is shown in figure 9. At a fixed time, c_f decreases sharply near the leading edge, then reaches zero and becomes negative. At a fixed x, c_f is nearly independent of time at smaller x's but decreases rather slowly at larger x's as t increases. A zero-c_f line separates, in the x,t-plane, the areas with positive and negative c_f respectively. The area of negative c_f calculated in the present problem is apparently very limited.

The displacement thickness Δ is shown in figure 10. At fixed times,

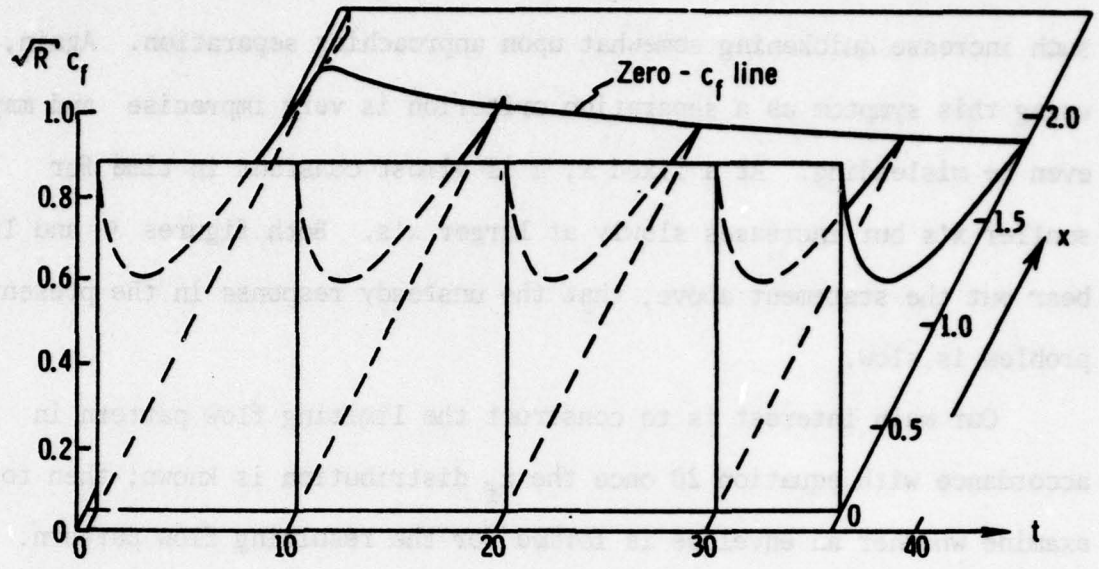

Figure 9. Skin friction distribution.

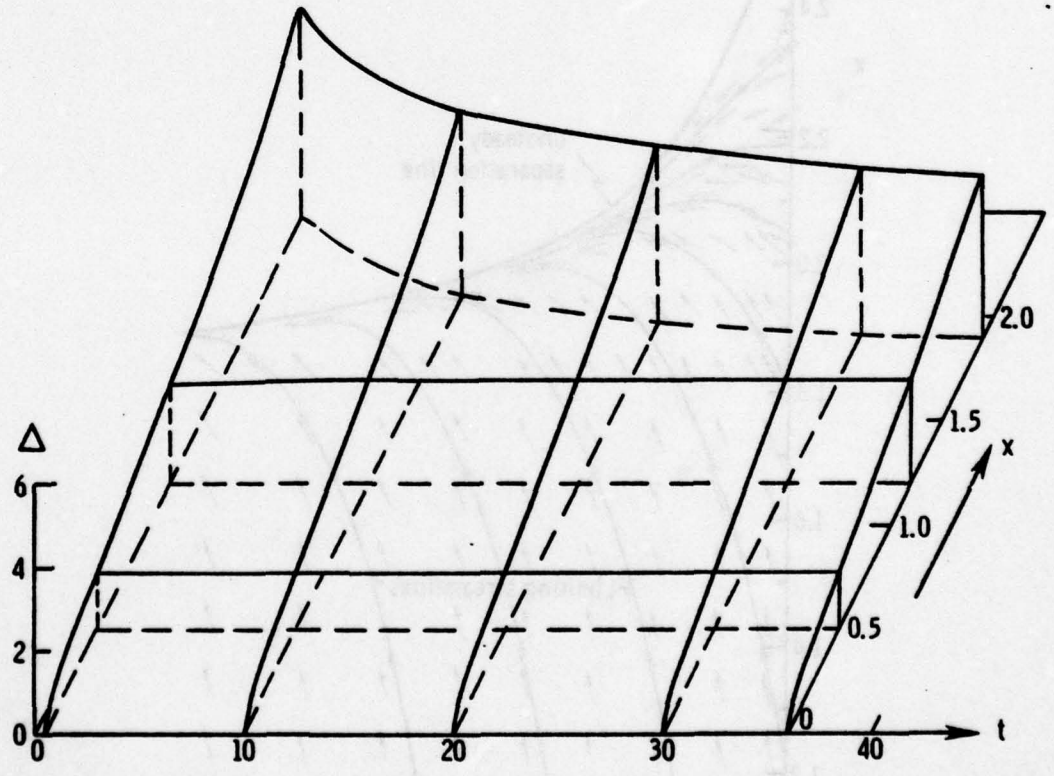

Figure 10. Displacement thickness distribution.

Δ increases from zero at the leading edge in the downstream, the rate of such increase quickening somewhat upon approaching separation. Again, using this symptom as a separation criterion is very imprecise and may even be misleading. At a fixed x, Δ is almost constant in time for smaller x's but increases slowly at larger x's. Both figures 9 and 10 bear out the statement above, that the unsteady response in the present problem is slow.

Our main interest is to construct the limiting flow pattern in accordance with equation 20 once the c_f distribution is known; then to examine whether an envelope is formed for the resulting flow pattern. Figure 11 shows the resultant flow pattern, where the arrows indicate the

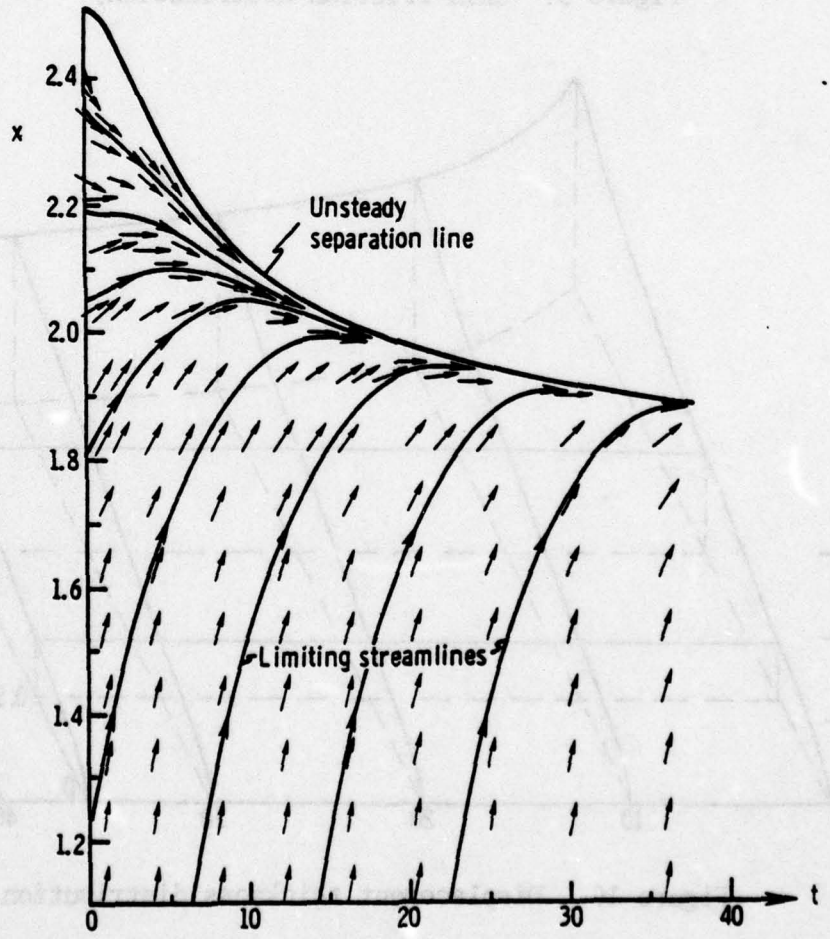

Figure 11. Limiting flow pattern and separation line.

local flow direction in the x,t-plane, and the solid lines drawn parallel to the arrows are the limiting streamlines. The expected envelope clearly appears at the top, starting from the initial steady-state separation point and asymptotically approaching the final steady state separation point. This envelope is referred to as the unsteady separation line. Since this line partitions the x,t-plane into two unconnected regions, the separation belongs to a "closed" type.

Some results of the present calcualtion are compared in figure 12 with those of Telionis and Tsahalis (1974a). There are agreements in some general trends, but discrepancies in others. The differences in the

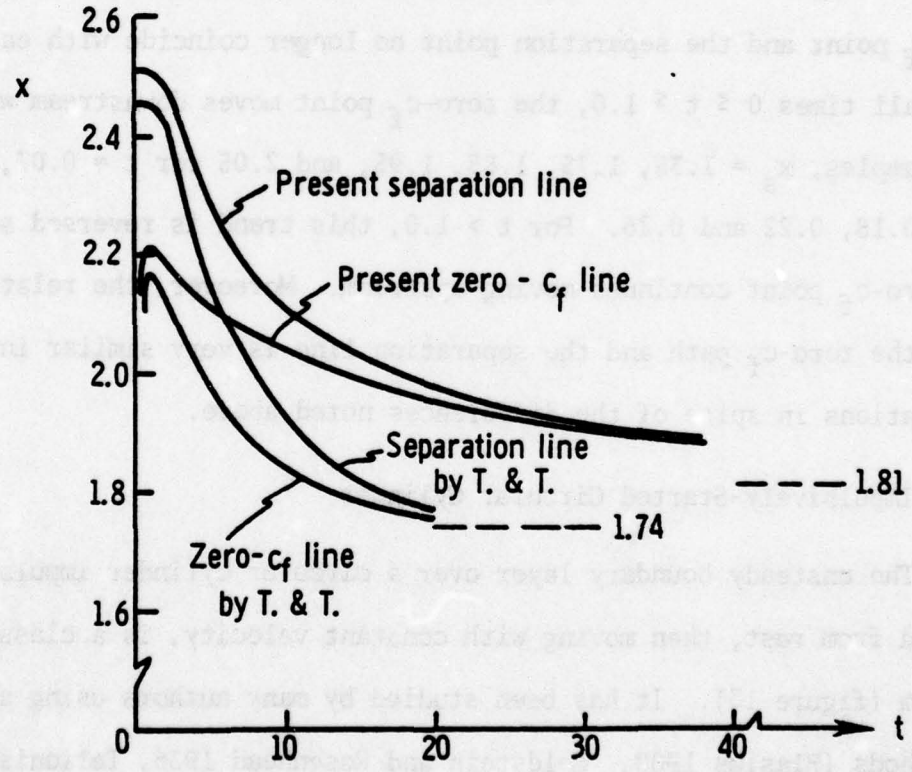

Figure 12. Comparison of zero-c_f line and separation line.

separation location at the initial and final steady-state were discussed above in connection with figure 8, but the main difference has to do with how the zero-c_f curves and the separation lines approach the asymptotic steady-state values. The Telionis and Tsahalis results indicate a much faster approach than ours. It is not clear what causes this difference, and especially puzzling is the fact that we have used the same computing program for the present Howarth's problem as we did for the cylinder problem (Section 3.3); however, our zero-c_f curve for the cylinder problem agrees extremely well with theirs (see figure 17).

Agreements are also noted in figure 12. Immediately after the impulsive change of the outer flow, the unsteady process takes over and the zero-c_f point and the separation point no longer coincide with each other. For small times $0 \leq t \leq 1.0$, the zero-c_f point moves downstream with time; for examples, $x_s = 1.35$, 1.75, 1.85, 1.95, and 2.05 for $t = 0.07$, 0.10, 0.14, 0.18, 0.22 and 0.26. For $t > 1.0$, this trend is reversed so that the zero-c_f point continues moving upstream. Moreover, the relation between the zero-c_f path and the separation line is very similar in both calculations in spite of the differences noted above.

3.3. Impulsively-Started Circular Cylinder

The unsteady boundary layer over a circular cylinder impulsively started from rest, then moving with constant velocity, is a classical problem (figure 13). It has been studied by many authors using a variety of methods (Blasius 1908, Goldstein and Rosenhead 1936, Telionis and Tsahalis 1974b, to name just a few). In comparison to the unsteady Howarth's problem discussed in the preceding section, the present one is

more common in practice, and more interesting with respect to the separation problem.

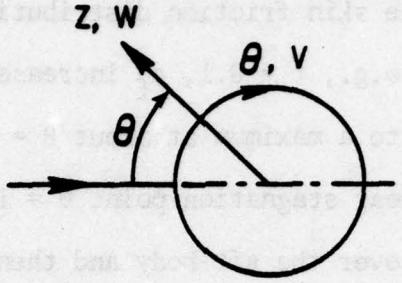

Figure 13. Circular cylinder.

Here the angular coordinate θ is used in place of x in equations 17 through 20, the metric coefficient $h_x = h_\theta = 1$, when nondimensionalized with the cylinder radius. Immediately after starting, the flow is inviscid with an outer velocity

$$V = 2 \sin\theta. \tag{25}$$

For the temporal initial profiles ($t = t_o$) the first approximation of a small-time expansion is adequate, i.e.

$$v(\theta,z,t_o) = V \operatorname{erf}\left(\frac{z}{2\sqrt{t_o}}\right), \tag{26}$$

where erf is the error function.

For the spatial initial profiles ($\theta=\theta_o$), solution of the steady, two-dimensional stagnation flow is valid; or equivalently the first approximation of the series expansion for steady boundary layer may be used. They are tabulated in standard texts (see Schlichting 1968).

The initial time t_o and space x_o were set at $t_o = 0.10$ and $\theta_o = 0.5°$, the time step Δt was 0.01, and the space step $\Delta\theta$ was 0.5°. The time range

of calculation extends to t = 2.3 at which the solutions appear to have reached the steady-state conditions.

Figure 14 shows the skin friction distribution in the θ,t-plane. At fixed initial times, e.g., t = 0.1, c_f increases from zero at the front stagnation point θ = 0° to a maximum at about θ = 80°, then gradually decreases to zero at the rear stagnation point θ = 180°. At fixed larger times, c_f falls to zero over the aft-body and then becomes negative.

On the other hand, at a fixed front-body station, e.g., θ = 40°, c_f decreases slowly for small times, but then remains constant at later times. This suggests that the front-body boundary layer reaches its steady-state condition very rapidly. In contrast, at a fixed aft-body station, e.g., θ = 120°, c_f falls rapidly with time and shows no sign of becoming steady within the present range of calculation. This reflects the idea that temporal development of the boundary layer is really confined to the rear body.

The area (in the θ, t-plane) with negative c_f is marked "reversed flow area." Following that is an "uncalculated area" which arises due to the zig-zag finite-difference scheme mentioned in Section 3.1. However, at the rear stagnation point θ = 180°, symmetry of flow requires c_f to be zero. Thus, one can reasonably conjecture that, in the "uncalculated area," c_f varies as indicated by the broken line along t = 0.9.

Large values of c_f appear at early times because, immediately after the impulsive start, vorticity is concentrated in a vortex sheet around the body, and c_f is theoretically everywhere infinite. Also, it should be noted that the rate at which c_f drops to zero increases with time, and is accompanied by a sharp increase in the displacement thickness (figure 15).

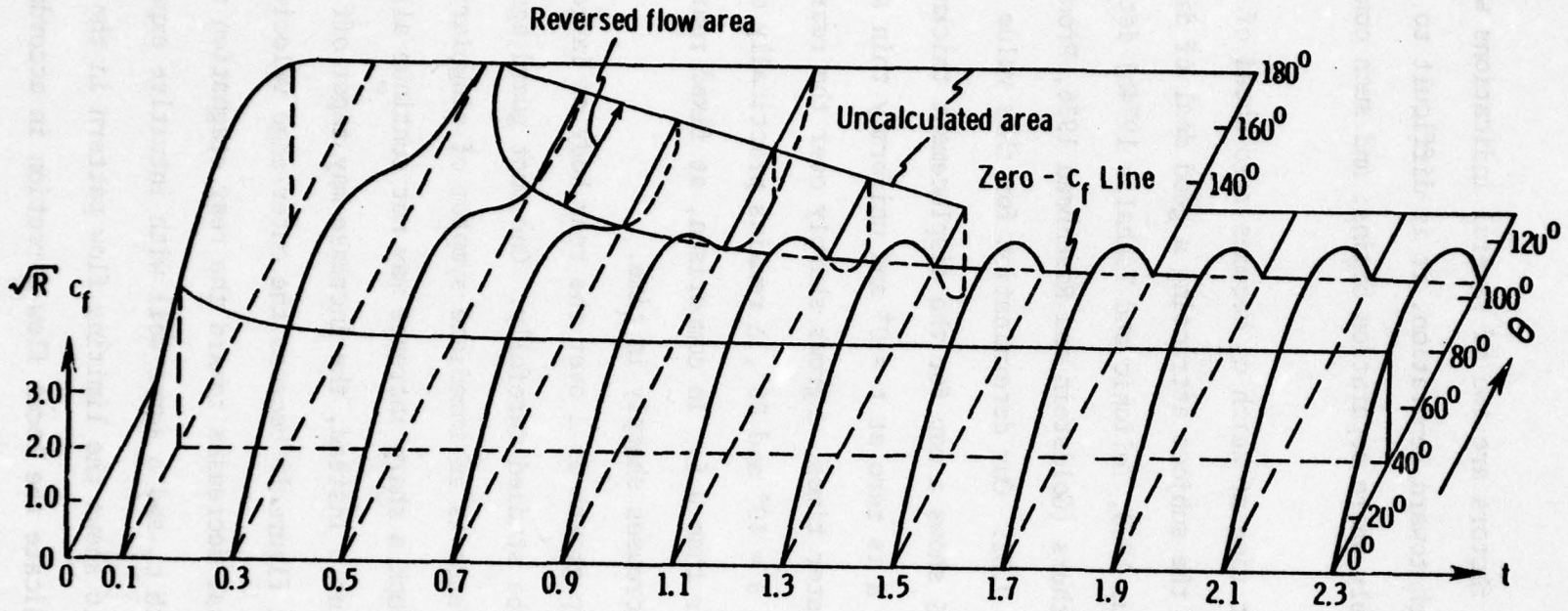

Figure 14. Skin friction distribution.

Although these factors are two of several indications which signal a gradual approach toward separation, it is difficult to define from these signals precisely where separation begins; and such conclusions can be misleading.

The first time at which c_f becomes zero ahead of the rear stagnation point has been the subject attracting a good deal of discussion. Some authors (Blasius 1908, Telionic and Tsahalis 1974b) determined this value as $t = 0.35$, others (Goldstein and Rosenhead 1936, Proudman and Johnson 1962) gave $t = 0.32$. Our determination for this value is 0.33.

Figure 15 shows a map for the displacement thickness Δ. At fixed initial times, Δ is zero at $t = 0^+$ and uniformly thin around the body at $t = 0.1$. At later times, Δ grows sharply over the rear body. At fixed space stations $\theta = 40°$ and $80°$, Δ remains practically constant for t roughly greater than 0.5. In comparison, at fixed rear-body stations, e.g., $\theta = 120°$, Δ increases sharply in time.

The sharp growth of Δ over the rear body at large times, such as $t = 1.3$, should be studied carefully. One must guard against concluding that the sharp increase is an immediate symptom of singularity and, hence, flow separation. Such a sharp increase may not continue all the way to the rear stagnation point. Instead, the increase may taper off as indicated by the broken line in figure 15 because the outer-edge velocity as well as the extent of reversal decreases toward the rear stagnation region. In any event, results of both c_f and Δ agree well with intuitive expectations.

Figure 16 shows the limiting flow pattern in the θ,t-plane. Again the arrows indicate the local flow direction in accordance with equation 20.

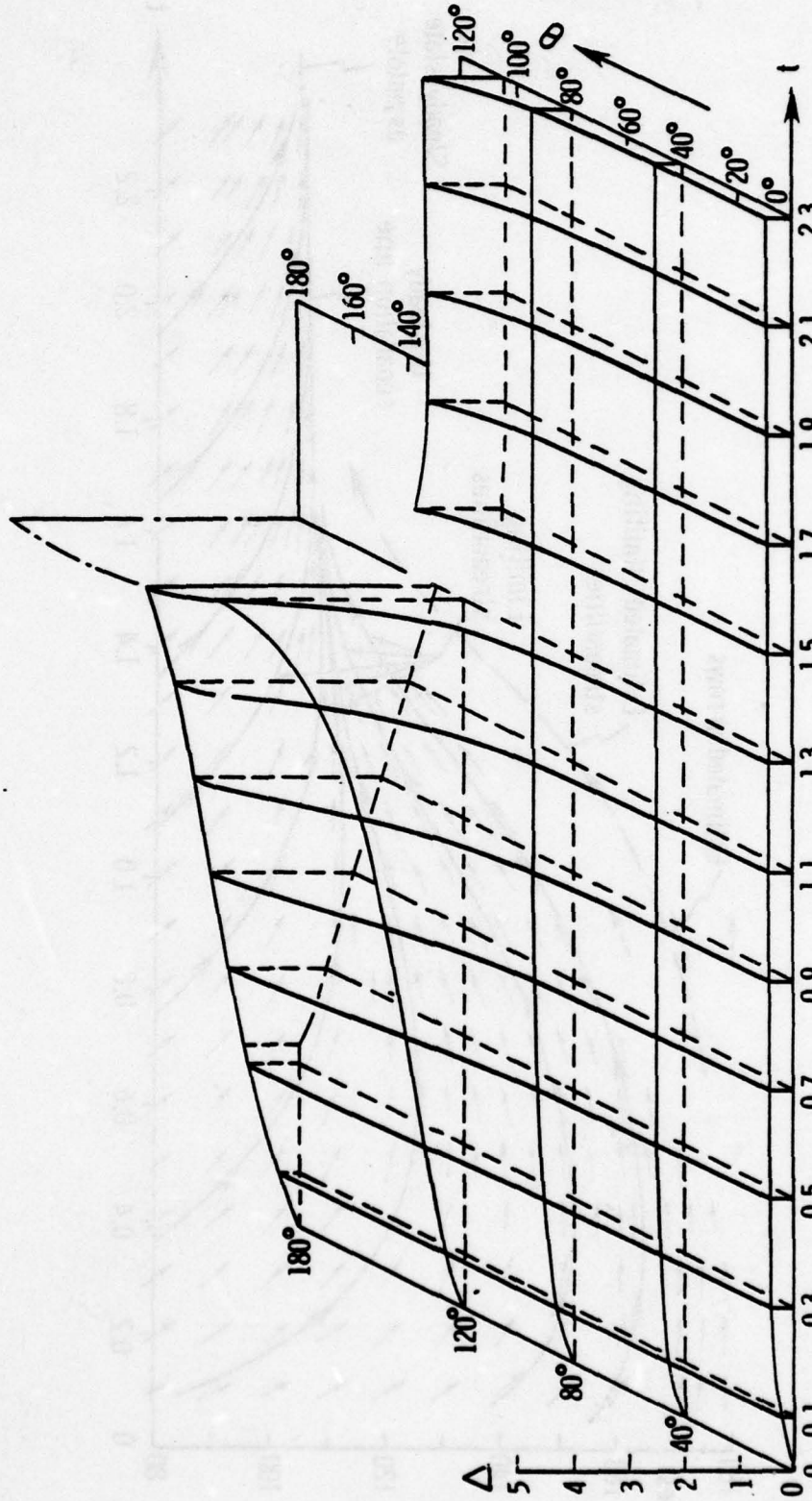

Figure 15. Displacement thickness distribution.

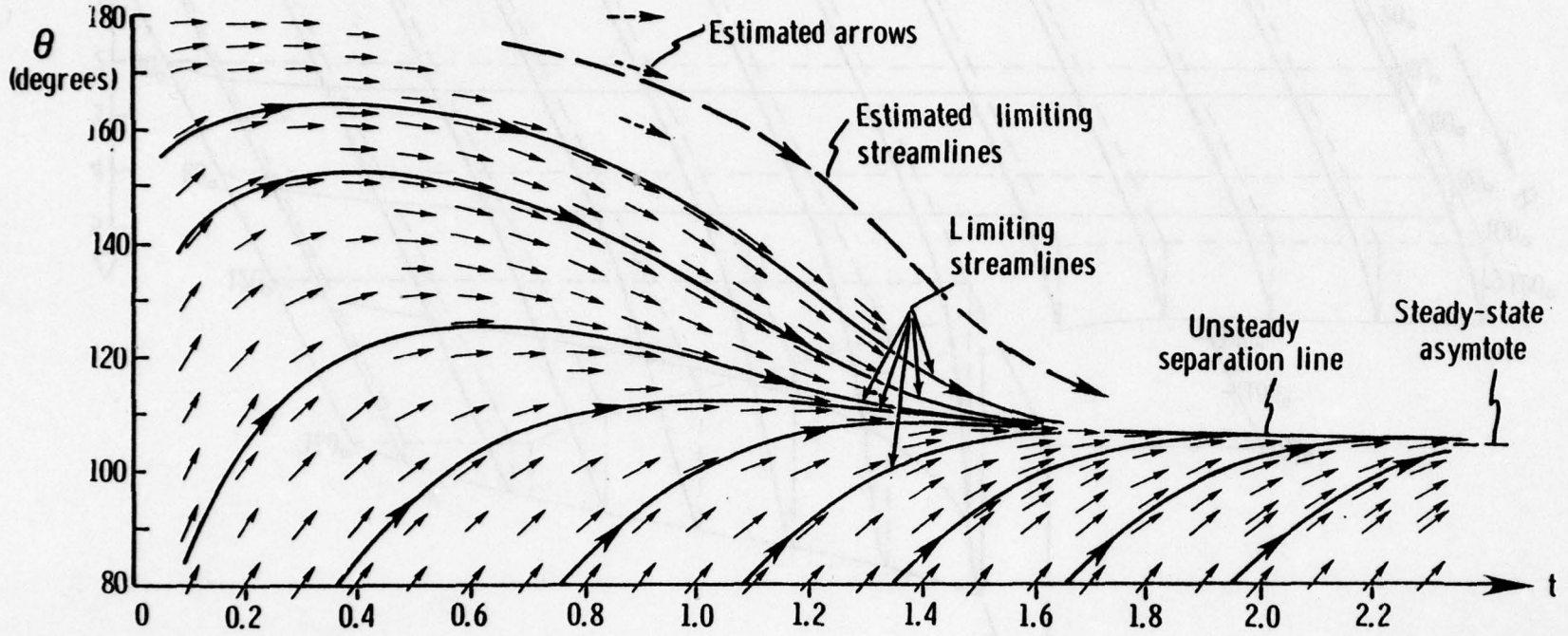

Figure 16. Limiting flow pattern and separation line.

The solid lines drawn parallel to the arrows are the analogous limiting streamlines. The crux of the matter here is to check whether an envelope is formed to these limiting streamlines. It is somewhat surprising that for a rather long time, roughly $t = 1.7$ (i.e., in the physical form, $t \sim 1.7\ a/V_\infty$ where a is the cylinder's radius), there is no sign of any envelope formation. Starting from $t \simeq 1.7$ an envelope appears to become visible, but it is still difficult to pinpoint the precise starting time. It may be $t = 1.65$, 1.75, or 1.80.

Based on our proposed criterion, we are led to conclude that no separation occurs prior to $t \simeq 1.7$, and that the envelope emerging thereafter can be designated as the separation line. The latter gives separation at $\theta = 105°$, when $t = 2.3$, which differs very little from asymptotic steady-state value of 104.5° given by Terrill (1960).

In the uncalculated area (figure 16), an estimated limiting streamline (represented by the broken lines) is inserted to indicate possible trends. This streamline is based on the estimated (broken) arrows, which, in turn, arise from the estimated negative c_f in figure 14. The open-type separation obtained is analogous to that for the steady three-dimensional case, because it is approached on both the upper and lower sides by the limiting streamlines originating from the front body at earlier times.

Figures 17 and 18 compare our results with those of Telionis and Tsahalis (1974b). Figure 17 shows that our zero-skin-friction line is in good agreement with that of Telionis and Tsahalis as well as with that of Thoman and Szewezyk (1969) from a Navier-Stokes solution. Figure 18 shows that Telionis and Tsahalis predicted a much earlier separation than we do. Our

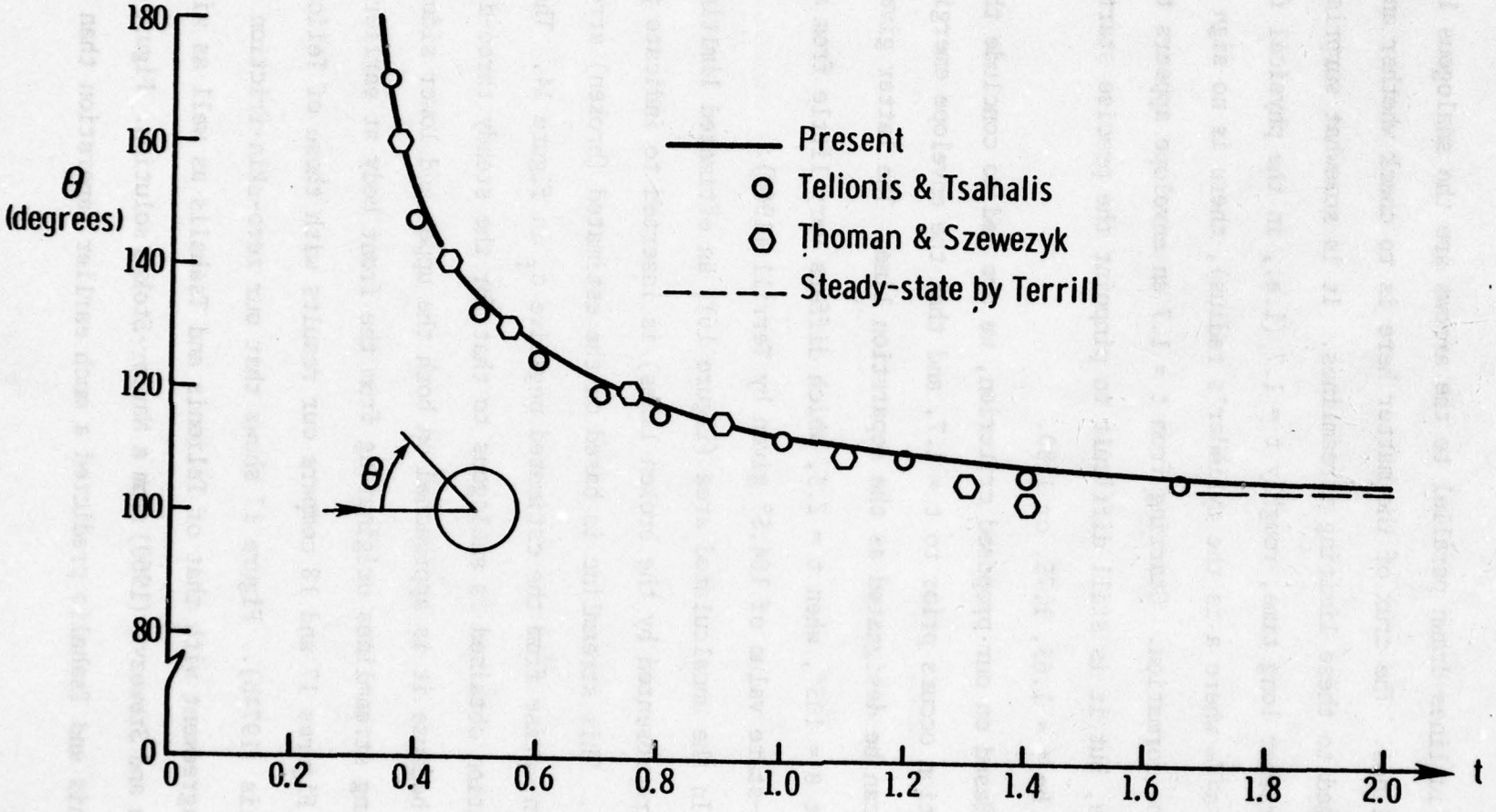

Figure 17. Comparison of zero-skin-friction lines.

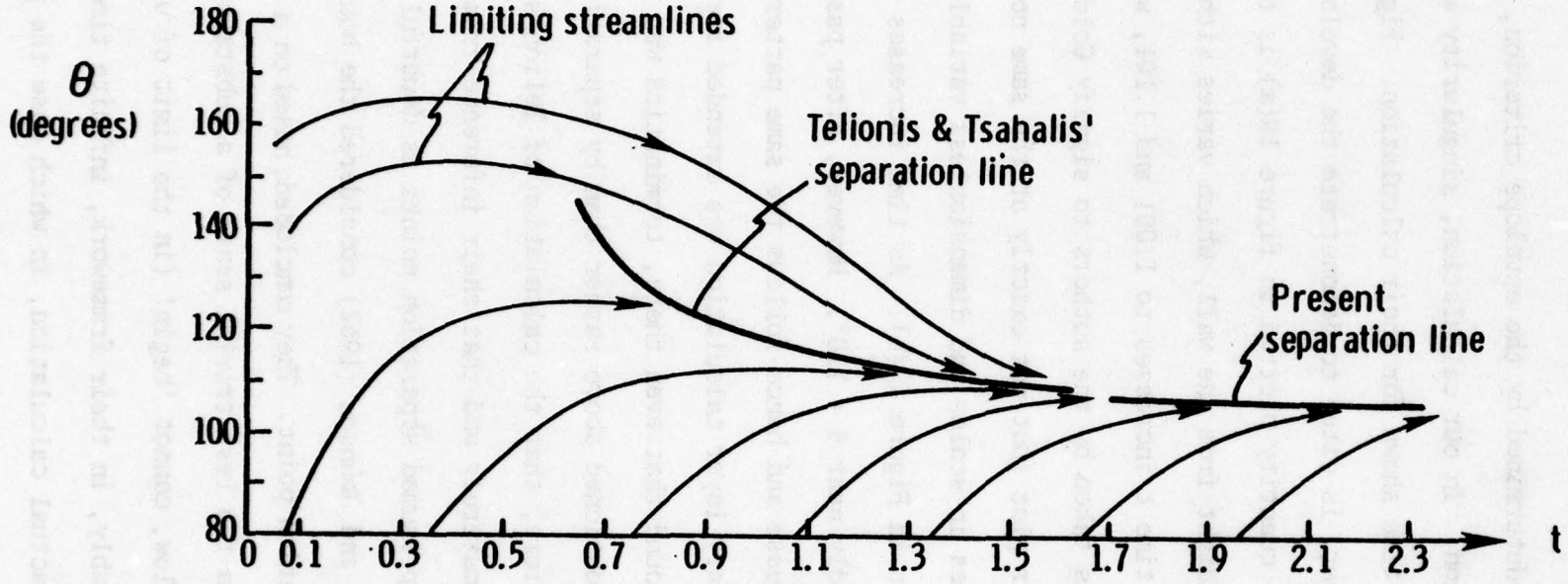

Figure 18. Comparison of separation lines.

separation is determined by the envelope criterion, theirs by the singularity criterion. In our calculation, singularity was not detected at the place and time shown for their calculation. Figure 19(a), reproduced from their paper, is cited to demonstrate the development of the singular behavior. The quantity plotted in figure 19(a) is the normal velocity, w, at a certain height from the wall, which varies with time around the cylinder. As time t increases to 1.001 and 1.101, w increases very sharply. This effect was taken by the authors to signify Goldstein's singularity.

A similar plot (but not exactly at the same normal distance, and with differences in scales and dimensionless variables) based on our calculation is shown in Figure 19(b). As time increases to t = 1.106, w indeed increases rapidly near $\theta = 110°$. However, after passing a peak value, w starts to decrease and hence follows the same pattern as for smaller t. When the boundary layer calculation was extended farther downstream, to $\theta = 140°$, we found that even there, termination was caused by the lack of initial data mentioned above rather than by separation phenomena. It appears, therefore, that the calculation of Telionis and Tsahalis was terminated prematurely and that their inference from the Goldstein singularity at the presumed separation points is doubtful.

Proudman and Johnson (1962) considered the boundary layer growth near the rear stagnation point. They concluded, based on a scaling argument, that "separation, in the less trivial sense of a substantial modification of the external flow, cannot 'begin' (in the limit of $\nu \to 0$) at any finite time." Presumably, in their framework, infinite time could mean some large instant in an actual calculation, in which case the present prediction of separation only after a long time appears to agree generally with Proudman and Johnson.

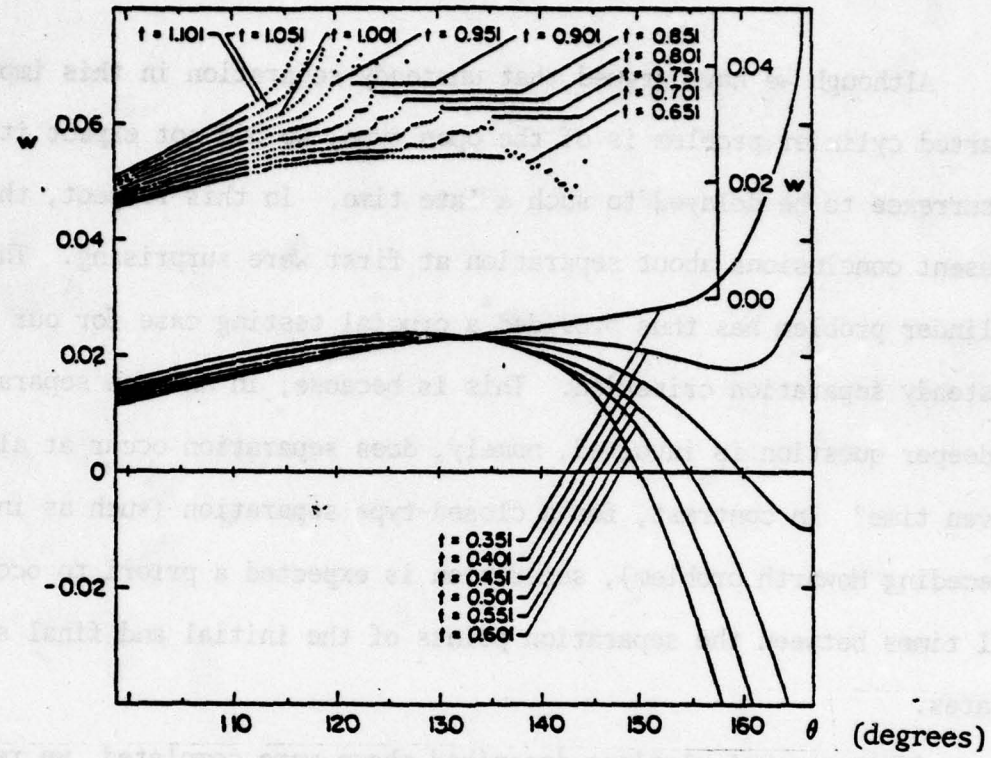

Figure 19(a). Normal velocity at η=0.1 (from Telionis and Tsahalis, 1974b). The scale on the left corresponds to t ≤0.601.

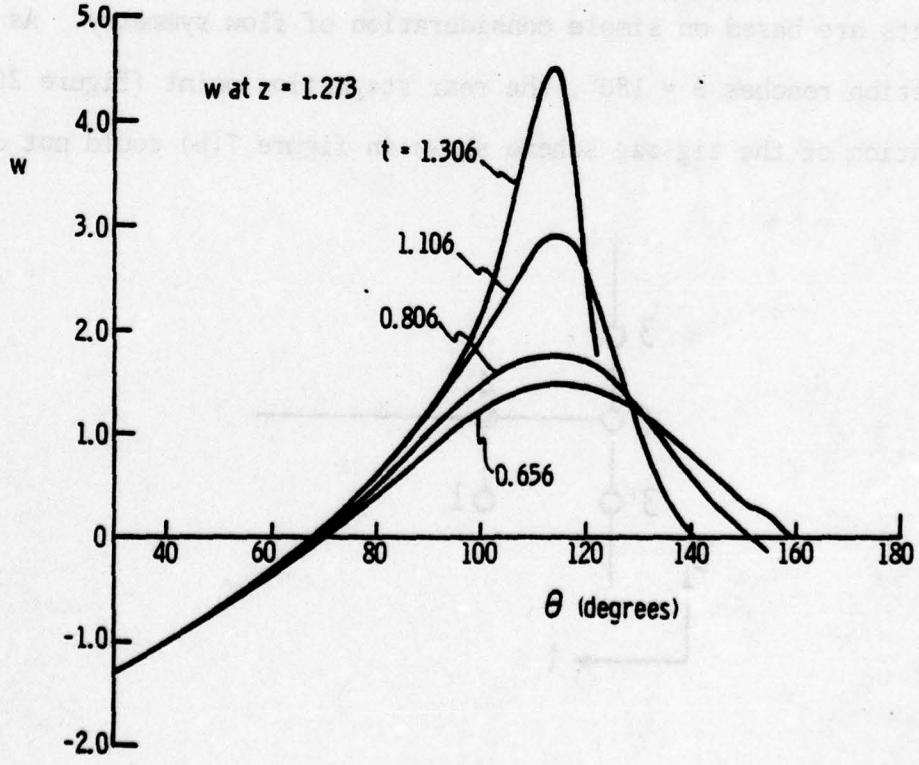

Figure 19(b). Normal velocity at z = 1.273.

Although we have argued that unsteady separation in this impulsively-started cylinder problem is of the open type, we did not expect its occurrence to be delayed to such a late time. In this respect, the present conclusions about separation at first were surprising. The present cylinder problem has thus provided a crucial testing case for our proposed unsteady separation criterion. This is because, in an open separation, a deeper question is involved, namely, does separation occur at all for a given time? In contrast, for a closed-type separation (such as in the preceding Howarth problem), separation is expected a priori to occur at all times between the separation points of the initial and final steady states.

After the calculations described above were completed, we realized that the preceding "uncalculated area" actually could be calculated. The arguments are based on simple consideration of flow symmetry. As the computation reaches $\theta = 180°$, the rear stagnation point (figure 20), application of the zig-zag scheme shown in figure 7(b) could not determine

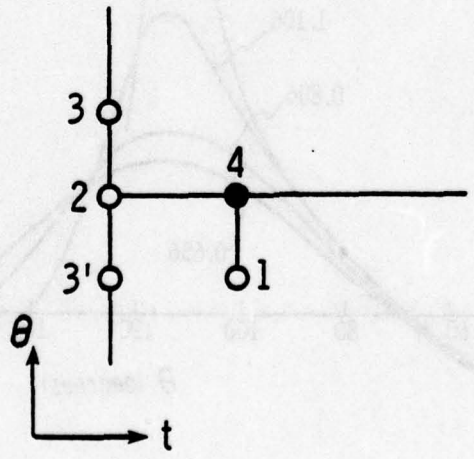

Figure 20. Computation at the rear stagnation point.

point 4 in figure 20 because point 3 is outside of the computation domain. However, in the present case (but not true for the Howarth problem discussed above), since flow is symmetric at $\theta = 180°$, solutions at point 3 are the same at the known point 3' except for a sign difference. Thus point 4 can be calculated, and employment of the zig-zag scheme does not necessarily prevent computation from being continued up to $\theta = 180°$ at all times. It is clear that, at $\theta = 180°$, the parallel velocity v is identically zero, but $\partial v/\partial\theta$ is nonvanishing, so that the continuity equation

$$\frac{\partial v}{\partial \theta} + \frac{\partial w}{\partial z} = 0 ,$$

enables one to determine a nontrivial normal velocity w.

4. UNSTEADY SEPARATION IN THREE DIMENSIONS

4.1 Proposed Separation Criterion

The unsteady separation criterion for three-dimensional flows can be derived in two ways: 1) from an extension of three-dimensional, steady separation criterion, and 2) from the two dimension unsteady separation criterion. For the convenience of reference, let the first be referred to as the time-fixed representation and the second, the space-fixed representation.

4.1.1 Time-fixed representation

For the unsteady, three-dimensional case, it is intuitive to look for an envelope of the limiting streamlines at each instant of time. In other words, we apply the envelope criterion for the steady, three-dimensional separation at each instantaneous time. The instantaneous envelope will be taken as the instantaneous separation line, and connecting a sequence of such separation lines results in an unsteady separation surface.

To illustrate, consider a simple system consisting of the space coordinates x,y,z and the time t. x and y are parallel to and z is normal to the body, while u, v, and w are the velocities along x,y,z. Figure 21 depicts the body surface (represented by the x,y-plane) at $t = t_1$ and t_2. The lines AB and CD represent the corresponding instantaneous separation lines, and the surface ABCD signifies the unsteady separation surface in the x,y,t-space. The arrow-curves are instantaneous limiting streamlines. In the three-dimensional unsteady case, there is the question of open versus closed separation in both the t-fixed and x- or y-fixed planes.

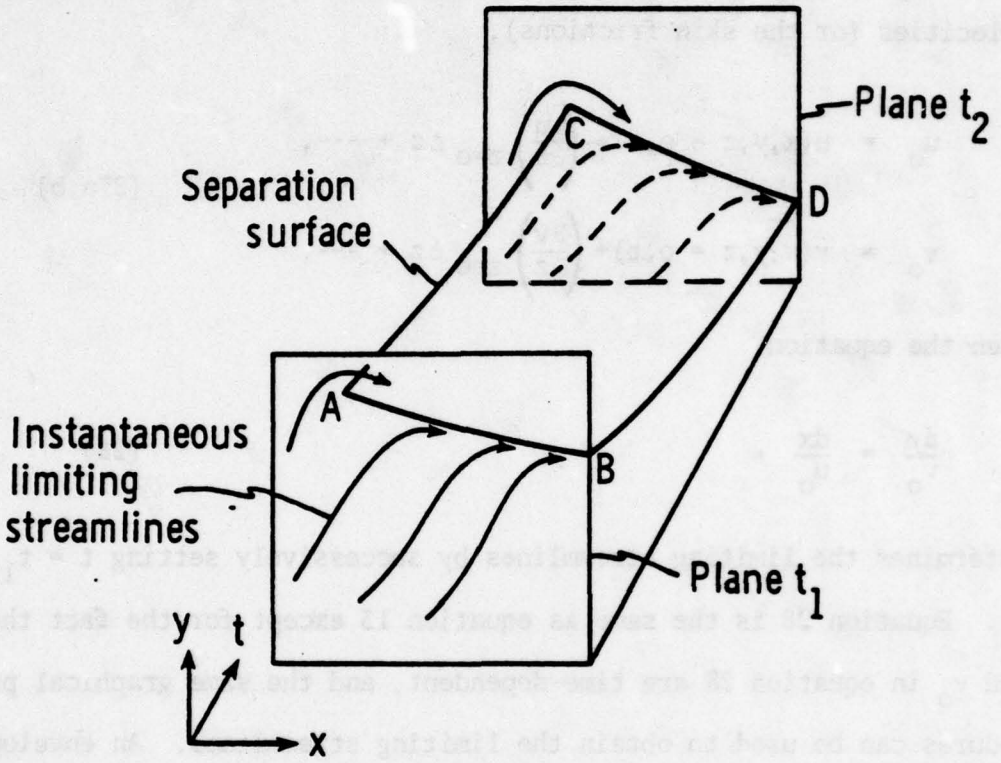

Figure 21. t-fixed representation of three-dimensional unsteady separation.

(In figure 21, an open separation in the x,y-plane is shown).

It should be clear that such a presentation of separation can be readily realized in experiment if one photographs the surface-flow pattern at successive times.

To construct the unsteady separation surface shown in figure 21, the boundary layer solution must be obtained first to yield the limiting velocities (or the skin frictions),

$$u_o = u(x,y,z=o,t) + \left(\frac{\partial u}{\partial z}\right)_{z=o} \Delta z + \text{---},$$
$$v_o = v(x,y,z=o,t) + \left(\frac{\partial v}{\partial z}\right)_{z=o} \Delta z + \text{---}. \qquad (27a,b)$$

Then the equation

$$\frac{dy}{v_o} = \frac{dx}{u_o}\ , \qquad (28)$$

determines the limiting streamlines by successively setting $t = t_1, t_2, \ldots t_n$. Equation 28 is the same as equation 13 except for the fact that u_o and v_o in equation 28 are time-dependent, and the same graphical procedures can be used to obtain the limiting streamlines. An envelope of these limiting streamlines then becomes the instantaneous separation line, such as lines AB and CD in figure 21. Connecting the successive instantaneous separation lines in the xyt-space gives a separation surface such as ABCD in the figure.

One should not confuse this description of determining an unsteady separation with a quasi-steady approximation. The crucial distinction is that we are not advocating a solution to the unsteady boundary layer equation by successively setting t equal to some constant. Instead, the full unsteady equations are first solved exactly to determine the unsteady velocity profiles u(x,y,z,t) and v(x,y,z,t), from which u_o and v_o are to be obtained. This prescribed procedure really amounts to a choice to

present the results of the limiting surface-flow pattern in succession of time. This procedure is obviously not different from taking surface-flow pattern pictures in an unsteady experiment at successively instants of time.

4.1.2. Space-fixed representation

In the above t-fixed representation, we confine our attention to the t-fixed planes, which is the usual experimental way of observing the flow. This is certainly a strong advantage; however, it is equally valid to consider the same problem by confining our attention to the successive x-constant planes, figure 22 (similarly for the y-constant planes).

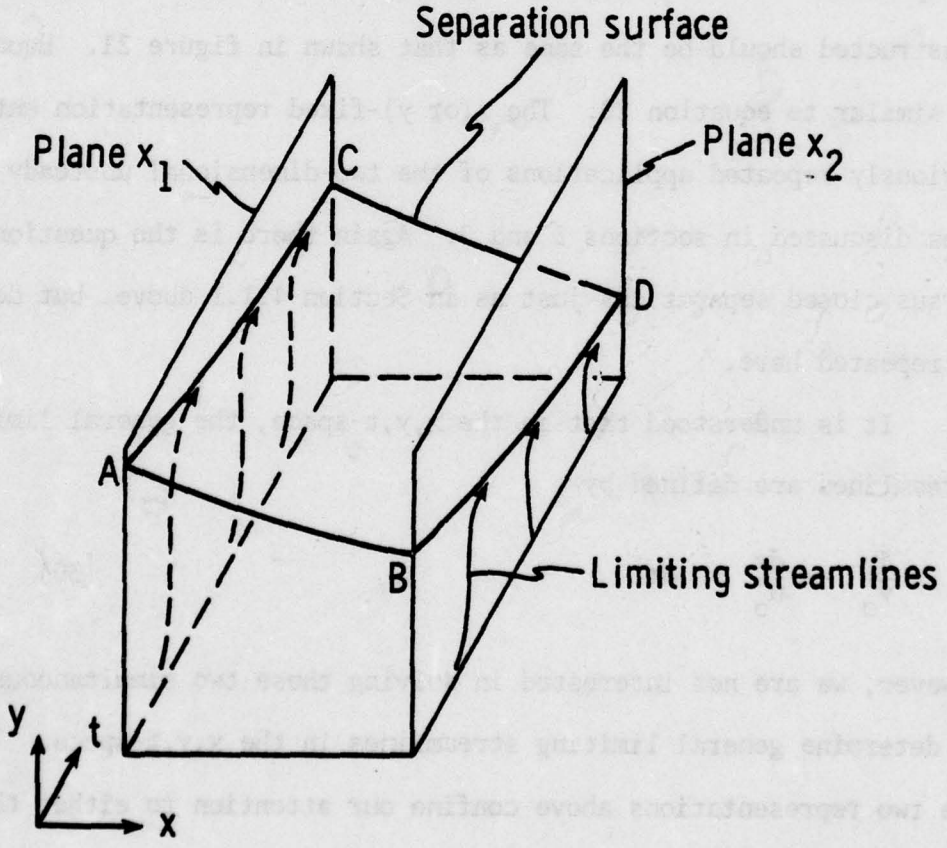

Figure 22. x-fixed representation of three dimensional unsteady separation.

Admittedly, it is difficult to simulate this procedure in an experiment, but there is no logical preference of the present representation to the preceding one. Using the relation

$$\frac{dy}{v_o} = dt \ , \tag{29}$$

one can construct the limiting streamlines in the x-fixed planes such as those shown in figure 22. If envelopes like AC and BD are formed by the limiting streamlines, these envelopes can be analogously taken as the separation lines. Connecting all such separation lines results again in a separation surface in the xyt-space, and the separation surface thus constructed should be the same as that shown in figure 21. Equation 29 is similar to equation 20. The x(or y)-fixed representation entails obviously repeated applications of the two-dimensional unsteady separation idea discussed in sections 2 and 3. Again there is the question of open versus closed separations just as in Section 4.1.1 above, but details are not repeated here.

It is understood that in the x,y,t-space, the general limiting streamlines are defined by

$$\frac{dy}{v_o} = \frac{dx}{u_o} = dt. \tag{30}$$

However, we are not interested in solving these two simultaneous equations to determine general limiting streamlines in the x,y,t-space. Instead, the two representations above confine our attention to either the t-fixed or the x-fixed planes. The result of separation should be the same whether equation 28, 29 or 30 is used.

We have illustrated that a three-dimensional, unsteady separation criterion can be obtained from repeated applications of either the steady, three-dimensional separation criterion or the unsteady, two-dimensional separation criterion. Conversely, we may say that our proposed unsteady separation criterion for three-dimensional flows is general, and logically includes both the known steady, three-dimensional separation criterion and the unsteady, two-dimensional separation criterion discussed in Sections 2 and 3 as special cases. On the other hand, the extension of the MRS criterion or the Goldstein singularity criterion has yet to be demonstrated.

4.2. Eichelbrenner's unsteady criterion

Eichelbrenner (1971) also discussed the question of unsteady separation in three dimensions. His main idea is expressed:

"...Thus we can define the unsteady separation line on the obstacle as the path of a unique (also instantaneous) stream surface on the obstacle, which passes through an instantaneous zero-friction point and separates the points of Groups I and II of the boundary layer." The points of Group I and II are further defined as those points connected by an instantaneous streamline at the stagnation point (or line), and those which are not connected to this point.

In a manner similar to our preceding discussion, Eichelbrenner's idea amounts to employing the steady-flow separation concept at each instant of time. However his concept of unsteady separation can be faulted for the same reason as his concept of steady separation (Eichelbrenner 1973),

namely, the characterization of the separation line passing through the zero-friction point and the division of points into I and II. These procedures apply only to the conventional kind of closed separation, but exclude the newer kind of open separation.

Eichelbrenner (1971) also states: "As the (instantaneous) separation surface of the external and internal points is approached, these streamlines become progressively tangential to this surface, which is thus itself a (unique) stream surface. Its path on the wall is then an instantaneous wall streamline delimiting wall streamlines at the exterior and interior of the separated zone. It is an asymptotic boundary of these lines (not an envelope)..."

Again his inference to the interior and exterior streamlines is valid only for the closed type of separation just noted. His emphasis that the separation line is itself a streamline, not an envelope, renews an old dispute. Earlier, Eichelbrenner advocated the envelope idea but apparently changed later to the streamline version. Lighthill (1963) first disputed the envelope version and suggested the streamline version. More recently, Legendre (1977) also concluded that he supported the streamline version. On the other hand, Stewartson and Brown (1968) have argued in favor of the envelope version discussed by Maskell (1955). Wang (1972) pointed out that Lighthill's definition of separation fits well with the conventional closed type of separation, but does not apply to the new open type of separation.

Analysis of isolated singularities such as nodal and saddle points (Lighthill 1963, Legendre 1977) and their combinations led to the conclusion that the separation line is a streamline distinguished from other

streamlines by its passing through the singular point. According to this version of separation, the limiting streamlines meet the separation line only at a nodal singularity.

On the other hand, based on the surface-flow visualization and recent limited calculated results, the limiting streamlines tend to come close together as they approach the separation line; or one may say, the limiting streamlines turn tangentially into the separation line. In particular the limiting streamlines do not appear to meet the separation line only at the nodal singularity, instead different limiting streamlines turn tangent to the separation line at different points along the latter. These features strongly suggest that the separation line is an envelope of the limiting streamlines. One clear advantage of the envelope definition of separation is that it applies to both open and closed separations. In our previous work, we have used this envelope version of separation.

By definition, envelope is a singular solution of the differential equation, say equation 13 or 20. So long as it is a solution, singular or regular, of the same limiting streamline equation, an envelope is certainly also a limiting streamline. At every point of the envelope, the flow is directed along the envelope. Hence there is nothing contradictory to call an envelope as a streamline. However, the streamline version of separation discussed above not only refers to the separation line as a limiting streamline, but also conceives that the separation line must pass through the singular points and meet the limiting streamline only at the nodal point. It is these latter features which do not hold in general.

The dispute between the streamline and the envelope definitions of separation is likely to continue presumably until more complete topological

surface-flow pictures over typical bodies become better understood and more rigorous studies near the separation line are available. Meanwhile the running-together of limiting streamlines as the physical characterization of separation (with the implication of vanishing normal skin friction) seems to be well accepted; Lighthill himself did not dispute this characterization although he objected to the envelope idea. For all intents and purposes, it appears that this particular feature alone is suffice to identifying separation in experiments as well as in calculations even though the search for a universally-agreed definition of separation may continue for some time to come.

5. CONCLUSIONS

It appears that the validity of the MRS criterion and the Goldstein singularity criterion for general unsteady flows remain unproven. Although the solutions of Williams and Johnson have demonstrated the MRS criterion, the special assumptions used there reduce the problems essentially to steady ones for which the validity of the MRS criterion has not been in doubt. The cylinder solution by Telionis and Tsahalis gave support to the Goldstein singularity criterion, but this solution was subsequently contradicted by later calculations. Apart from the basic validity question, both of these criteria are inconvenient to apply; in addition, their extension to three-dimensional case has not been shown.

The limiting streamlines and their envelope as the separation line for steady, three-dimensional boundary layers have been well demonstrated by experiments and to a lesser extent by calculations. These concepts are analogically applied here to the unsteady, two-dimensional case. Pertinent equations are formally transformed from one to the other; similar limiting streamlines are defined in the x,t-plane for the unsteady case; and the envelope of those limiting streamlines is proposed as a new unsteady separation criterion. This criterion determines separation without relying on usual symptoms such as rapid increase of boundary layer thickness, etc., and it is also consistent with the criterion for general unsteady separation in three dimensions discussed in this work.

Analogous to the three-dimensional, steady case, separation can also be classified as an open or a closed type for the two-dimensional, unsteady

case. The word "closed" or "open," means that the separation line as an envelope of the limiting streamlines does or does not divide the x,t-plane into two unconnected regions. To illustrate these types of separation, two previously studied examples have been recalculated. The first one - unsteady response to a sudden change of the Howarth steady problem presents a closed separation; the second one - unsteady growth of an impulsively started circular cylinder from rest - presents an open separation. The calculations were made through analogy using the existing computing codes previously developed for the steady, three-dimensional problems.

Results have been compared to those of Telionis and Tsahalis. For the first problem, agreements were noted in general trends of the separation line in relation to the zero-skin-friction line, but discrepancies are found in actual locations of these lines. Also their results show a much faster approach toward the final steady-state condition than ours. For the second problem, results of the zero-skin-friction agree very well, but those of the separation line are entirely different. Our separation is determined by the converging together or an envelope of the limiting streamlines, theirs by the singularity criterion. In our calculation, no singularity was detected at the place and time shown from their calculations. While they predicted a much earlier separation, we predicted separation occurring only at large times. Our separation prediction appears to be consistent with that of Proudman and Johnson.

General unsteady separation in three-dimensions has been described also. It is based on the application of steady three-dimensional criterion at successive instants of time. This simulates the usual sequence of

observing an unsteady flow, and does not necessarily imply a quasi-steady approach. Alternatively, it may be looked upon as applying the unsteady, two-dimensional criterion to staggering fixed coordinate planes. Hence the three-dimensional unsteady separation we propose here includes both the steady, three-dimensional separation and the unsteady, two-dimensional separation as special cases. Our unsteady, three-dimensional separation criterion differs from that of Eichelbrenner in that the latter contains only the closed type of separation, while it excludes the open type.

ACKNOWLEDGEMENT

The author wishes to acknowledge helpful discussions with M. Cooper, R. Cooper, S. H. Maslen and K. Stewartson. This work was supported by the Office of Naval Research under Contract N00014-77-C-0650.

6. REFERENCES

Blasius, H. (1908). Grenzschichten in Flüssigkeiten mit Kleiner Reibung. Z. Math. U. Phys. 56, 1-37. Eng. translation in NACA TM 1256.

Brown, S. N. (1965). Singularities associated with separating boundary layer. Philos. Trans. Roy. Soc. London Ser. A, 257, 409-444.

Cebeci, T. (1978). An unsteady laminar boundary layer with separation and reattachment. AIAA J. 16, 2, 1305-1306.

Dwyer, H. A. (1968). Calculation of unsteady leading-edge boundary layers. AIAA J. 6, 12, 2447-2448.

Eichelbrenner, E. A. (1971). Decollement Instationnaire en Regime Laminaire A Trois Dimensions. Recent Research on Unsteady Boundary Layers (Proc. May, 1971 Symposium of IUTAM), E. Eichelbrenner, ed., Laval University Press, Quebec, Vol. I, 609-636.

Eichelbrenner, E. A. (1973). Three-dimensional boundary layers, Annual Review of Fluid Mechanics, Annual Review Inc., Palo Alto, Calif., Vol. 5, 339-360.

Goldstein, S. and Rosenhead, L. (1936). Boundary layer growth. Proc. Cambridge Philos. Soc., 32, 392-401.

Goldstein, S. (1948). On laminar boundary-layer flow near a position of spearation. Quart. J. Mech. Appl. Math. 1, 43-69.

Hall, M. G. (1969). The boundary layer over an impulsively started flat plate. Proc. Roy. Soc. London Ser. A. 310, 401-414.

Howarth, L. (1938). On the solution of the laminar boundary layer equations. Proc. Roy. Soc. London Ser. A, 164, 547-549.

Krause, E., Hirschel, E. H. and Bothmann, Th. (1969). Die Numerische integration der bewegungsgleichungen dreidimensionaler Kompressibler grenzschichten. DGLR-Fachbuchreihe Band 3, Braunschweig, 03-43.

Maskell, E. C. (1955). Flow separation in three dimensions. RAE Rep. Aero. 2565, Royal Aircraft Establishment, Bedrord, England.

Patel, V. C. and Nash, J. F. (1971). Some solutions of the unsteady turbulent boundary layer equations. Recent Research on Unsteady Boundary Layers (Proc. May 1971 Symposium of IUTAM), Vol. I, E. A. Eichelbrenner, ed., Laval University Press, Quebec, 1106-1165.

Patel, V. C. and Nash, J. F. (1976). Recent advances in the calculation of turbulent boundarys: three dimensional and unsteady flows. Proc. of the Lockheed-Georgia Company Viscous Flow Symposium, LG 77ER0044, Atlanta, Ga., 291-340.

Phillips, J. H. and Ackerberg, R. C. (1973). A numerical method for integrating the unsteady boundary-layer equations when there are regions of backflow. J. Fluid Mech. 58, 561-579.

Proudman, I. and Johnson, K. (1962). Boundary-layer growth near a rear stagnation point. J. Fluid Mech. 12, 161-168.

Rott, N. (1956). Unsteady viscous flow in the vicinity of a stagnation point. Quart. Appl. Math. 13, 444-451.

Schlichting, H. (1969). Boundary Layer Theory, 6th Edition, McGraw Hill.

Sears, W. R. and Telionis, D. P. (1971). Unsteady boundary-layer separation. Recent Research on Unsteady Boundary Layers (Proc. May 1971 Symposium of IUTAM) Vol. 1, E. A. Eichelbrenner, ed., Laval University Press, Quebec. 404-447.

Sears, W. R. and Telionis, D. P. (1975). Boundary-layer separation in unsteady flow. SIAM J. Appl. Math. 28, 1, 215-235.

Stewartson, K. (1958). On Goldstein's theory of laminar separation. Q. J. Mech. Appl. Math. 11, 399-410.

Stewartson, K. (1960). The theory of unsteady laminar boundary layers. Advanced in Applied Mechanics 6. Academic Press, London, 349-408.

Stewartson, K. (1963). The Theory of Laminar Boundary Layers in Compressible Fluids. Oxford University Press, London.

Telionis, D. P. and Tsahalis, D. Th. (1974a). The response of unsteady boundary-layer separation to impulsive changes of outer flow. AIAA J., 12, 614-619.

Telionis, D. P. and Tsahalis, D. Th. (1974b). Unsteady laminar separation over impulsively moved cylinders. Acta Astronautica, 1, 1487-1505.

Terrill, R. M. (1960). Laminar boundary-layer flow near separation with and without suction. Phil. Trans. Roy. Soc. London, A 253, 55-100.

Thoman, D. C. and Szewczyk, A. A. (1969). Time-dependent viscous flow over a circular cylinder. Phys. of Fluids, Supplement II, 76-86.

Wang, K. C. (1970). Three-dimensional boundary layer near the plane of symmetry of a spheroid at incidence. J. Fluid Mech. 43, 1, 187-209.

Wang, K. C. (1971). On the determination of the zones of influence and dependence for three-dimensional boundary layer equations. J. Fluid Mech. 48, 2, 397-404.

Wang, K. C. (1972). Separation patterns of boundary layer over an inclined body of revolution. AIAA J., 10, 8, 1044-1050.

Wang, K. C. (1974). Boundary layer over a blunt body at high incidence with an open-type of separation. Proc. Roy. Soc. London Ser. A, 340, 33-55.

Wang, K. C. (1975a). Boundary layer over a blunt body at low incidence with circumferential reversed flow. J. Fluid Mech. 72, 1, 49-65.

Wang, K. C. (1975b). Aspects of "Multitime initial-value problem" originating from boundary layer equations. Phys. of Fluids, 18, 8, 951-955.

Wang, K. C. (1976). Separation of three-dimensional flow. Proc. of the Lockheed-Georgia Company Viscous Flow Symposium, LG77ER0044, Atlanta, Ga. 341-414. Also Martin Marietta Laboratories TR 76-54c, 1976.

Williams, J. C. III and Johnson, W. D. (1974a). Semi-similar solutions to unsteady boundary layer flows including separation. AIAA J. 12, 1388-1393.

Williams, J. C. III and Johnson, W. D. (1974b). Note on unsteady boundary-layer separation. AIAA J. 12, 1427-1429.

Williams, J. C. III (1977). Incompressible boundary-layer separation. Ann. Rev. Fluid Mech. 9, 113-144.

DISTRIBUTION LIST FOR UNCLASSIFIED
TECHNICAL REPORTS AND REPRINTS ISSUED UNDER
CONTRACT N00014-77-C-0650 TASK NR 061-352

All addresses receive one copy unless otherwise specified

Technical Library
Building 313
Ballistic Research Laboratories
Aberdeen Proving Ground, MD 21005

Dr. F. D. Bennett
External Ballistic Laboratory
Ballistic Research Laboratories
Aberdeen Proving Ground, MD 21005

Mr. C. C. Hudson
Sandia Corporation
Sandia Base
Albuquerque, NM 81115

Professor P. J. Roache
Ecodynamics Research
Associates, Inc.
P. O. Box 8172
Albuquerque, NM 87108

Dr. J. D. Shreve, Jr.
Sandia Corporation
Sandia Base
Albuquerque, NM 81115

Defense Documentation Center
Cameron Station, Building 5
Alexandria, VA 22314 12 copies

Library
Naval Academy
Annapolis, MD 21402

Director, Tactical Technology Office
Defense Advanced Research Projects
Agency
1400 Wilson Boulevard
Arlington, VA 22209

Office of Naval Research
Attn: Code 211
800 N. Quincy Street
Arlington, VA 22217

Office of Naval Research
Attn: Code 438
800 N. Quincy Street
Arlington, VA 22217

Office of Naval Research
Attn: Code 1021P (ONRL)
800 N. Quincy Street
Arlington, VA 22217 6 copies

Dr. J. L. Potter
Deputy Director, Technology
von Karman Gas Dynamics Facility
Arnold Air Force Station, TN 37389

Professor J. C. Wu
Georgia Institute of Technology
School of Aerospace Engineering
Atlanta, GA 30332

Library
Aerojet-General Corporation
6352 North Irwindale Avenue
Azusa, CA 91702

NASA Scientific and Technical
Information Facility
P. O. Box 8757
Baltimore/Washington International
Airport, MD 21240

Dr. K. C. Wang
Martin Marietta Corporation
Martin Marietta Laboratories
1450 South Rolling Road
Baltimore, MD 21227

Dr. S. A. Berger
University of California
Department of Mechanical Engineering
Berkeley, CA 94720

Professor A. J. Chorin
University of California
Department of Mathematics
Berkeley, CA 94720

Professor M. Holt
University of California
Department of Mechanical Engineering
Berkeley, CA 94720

Dr. H. R. Chaplin
Code 1600
David W. Taylor Naval Ship Research
and Development Center
Bethesda, MD 20084

Dr. Hans Lugt
Code 184
David W. Taylor Naval Ship Research
and Development Center
Bethesda, MD 20084

Dr. Francois Frenkiel
Code 1802.2
David W. Taylor Naval Ship Research
and Development Center
Bethesda, MD 20084

Dr. G. R. Inger
Department of Aerospace Engineering
Virginia Polytechnic Institute and
State University
Blacksburg, VA 24061

Professor A. H. Nayfeh
Department of Engineering Science
Virginia Polytechnic Institute and
State University
Blacksburg, VA 24061

Mr. A. Rubel
Research Department
Grumman Aerospace Corporation
Bethpage, NY 11714

Commanding Officer
Office of Naval Research Branch Office
666 Summer Street, Bldg. 114, Section D
Boston, MA 02210

Dr. G. Hall
State University of New York at Buffalo
Faculty of Engineering and Applied
Sciences
Fluid and Thermal Sciences Laboratory
Buffalo, NY 14214

Dr. R. J. Vidal
CALSPAN Corporation
Aerodynamics Research Department
P. O. Box 235
Buffalo, NY 14221

Professor R. F. Probstein
Department of Mechanical Engineering
Massachusetts Institute of Technology
Cambridge, MA 02139

Commanding Officer
Office of Naval Research Branch Office
536 South Clark Street
Chicago, IL 60605

Code 753
Naval Weapons Center
China Lake, CA 93555

Mr. J. Marshall
Code 4063
Naval Weapons Center
China Lake, CA 93555

Professor R. T. Davis
Department of Aerospace Engineering
University of Cincinnati
Cincinnati, OH 45221

Library MS 60-3
NASA Lewis Research Center
21000 Brookpark Road
Cleveland, OH 44135

Dr. J. D. Anderson, Jr.
Chairman, Department of Aerospace
Engineering
College of Engineering
University of Maryland
College Park, MD 20742

Professor W. L. Melnik
Department of Aerospace Engineering
University of Maryland
College Park, MD 20742

Professor O. Burggraf
Department of Aeronautical and
Astronautical Engineering
Ohio State University
1314 Kinnear Road
Columbus, OH 43212

Technical Library
Naval Surface Weapons Center
Dahlgren Laboratory
Dahlgren, VA 22448

Dr. F. Moore
Naval Surface Weapons Center
Dahlgren Laboratory
Dahlgren, VA 22448

Technical Library 2-51131
LTV Aerospace Corporation
P. O. Box 5907
Dallas, TX 75222

Library, United Aircraft Corporation
Research Laboratories
Silver Lane
East Hartford, CT 06108

Technical Library
AVCO-Everett Research Laboratory
2385 Revere Beach Parkway
Everett, MA 02149

Professor G. Moretti
Polytechnic Institute of New York
Long Island Center
Department of Aerospace Engineering
and Applied Mechanics
Route 110
Farmingdale, NY 11735

Professor S. G. Rubin
Polytechnic Institute of New York
Long Island Center
Department of Aerospace Engineering
and Applied Mechanics
Route 110
Farmingdale, NY 11735

Dr. W. R. Briley
Scientific Research Associates, Inc.
P. O. Box 498
Glastonbury, CT 06033

Professor P. Gordon
Calumet Campus
Department of Mathematics
Purdue University
Hammond, IN 46323

Library (MS 185)
NASA Langley Research Center
Langley Station
Hampton, VA 23665

Professor A. Chapmann
Chairman, Mechanical Engineering
Department
William M. Rice Institute
Box 1892
Houston, TX 77001

Technical Library
Naval Ordnance Station
Indian Head, MD 20640

Professor D. A. Caughey
Sibley School of Mechanical and
Aerospace Engineering
Cornell University
Ithaca, NY 14850

Professor E. L. Resler
Sibley School of Mechanical and
Aerospace Engineering
Cornell University
Ithaca, NY 14850

Professor S. F. Shen
Sibley School of Mechanical and
Aerospace Engineering
Ithaca, NY 14850

Library
Midwest Research Institute
425 Volker Boulevard
Kansas City, MO 64110

Dr. M. M. Hafez
Flow Research, Inc.
P. O. Box 5040
Kent, WA 98031

Dr. E. M. Murman
Flow Research, Inc.
P. O. Box 5040
Kent, WA 98031

Dr. S. A. Orszag
Cambridge Hydrodynamics, Inc.
54 Baskin Road
Lexington, MA 02173

Dr. P. Bradshaw
Imperial College of Science and
Technology
Department of Aeronautics
Prince Consort Road
London SW7 2BY, England

Professor T. Cebeci
California State University,
LongBeach
Mechanical Engineering Department
Long Beach, CA 90840

Mr. J. L. Hess
Douglas Aircraft Company
3855 Lakewood Boulevard
Long Beach, CA 90808

Dr. H. K. Cheng
University of Southern California,
University Park
Department of Aerospace Engineering
Los Angeles, CA 90007

Professor J. D. Cole
Mechanics and Structures Department
School of Engineering and Applied
Science
University of California
Los Angeles, CA 90024

Engineering Library
University of Southern California
Box 77929
Los Angeles, CA 90007

Dr. C. -M. Ho
Department of Aerospace Engineering
University of Southern California,
University Park
Los Angeles, CA 90007

Dr. T. D. Taylor
The Aerospace Corporation
P. O. Box 92957
Los Angeles, CA 90009

Commanding Officer
Naval Ordnance Station
Louisville, KY 40214

Mr. B. H. Little, Jr.
Lockheed-Georgia Company
Department 72-74, Zone 369
Marietta, GA 30061

Professor E. R. G. Eckert
University of Minnesota
241 Mechanical Engineering Building
Minneapolis, MN 55455

Library
Naval Postgraduate School
Monterey, CA 93940

Supersonic-Gas Dynamics Research
Laboratory
Department of Mechanical Engineering
McGill University
Montreal 12, Quebec, Canada

Dr. S. S. Stahara
Nielsen Engineering & Research, Inc.
510Clyde Avenue
Mountain View, CA 94043

Engineering Societies Library
345 East 47th Street
New York, NY 10017

Professor A. Jameson
New York University
Courant Institute of Mathematical
Sciences
251 Mercer Street
New York, NY 10012

Professor G. Miller
Department of Applied Science
New York University
26-36 Stuyvesant Street
New York, NY 10003

Office of Naval Research
New York Area Office
715 Broadway - 5th Floor
New York, NY 10003

Dr. A. Vaglio-Laurin
Department of Applied Science
26-36 Stuyvesant Street
New York University
New York, NY 10003

Professor H. E. Rauch
Ph.D. Program in Mathematics
The Graduate School and University
Center of the City University of
New York
33 West 42nd Street
New York, NY 10036

Librarian, Aeronautical Library
National Research Council
Montreal Road
Ottawa 7, Canada

Lockheed Missiles and Space Company
Technical Information Center
3251 Hanover Street
Palo Alto, CA 94304

Commanding Officer
Office of Naval Research Branch Office
1030 East Green Street
Pasadena, CA 91106

California Institute of Technology
Engineering Division
Pasadena, CA 91109

Library
Jet Propulsion Laboratory
4800 Oak Grove Drive
Pasadena, CA 91103

Professor H. Liepmann
Department of Aeronautics
California Institute of Technology
Pasadena, CA 91109

Mr. L. I. Chasen, MGR-MSD Lib.
General Electric Company
Missile and Space Division
P. O. Box 8555
Philadelphia, PA 19101

Mr. P. Dodge
Airesearch Manufacturing Company
of Arizona
Division of Garrett Corporation
402 South 36th Street
Phoenix, AZ 85010

Technical Library
Naval Missile Center
Point Mugu, CA 93042

Professor S. Bogdonoff
Gas Dynamics Laboratory
Department of Aerospace and
Mechanical Sciences
Princeton University
Princeton, NJ 08540

Professor S. I. Cheng
Department of Aerospace and
Mechanical Sciences
Princeton University
Princeton, NJ 08540

Dr. J. E. Yates
Aeronautical Research Associates
of Princeton, Inc.
50 Washington Road
Princeton, NJ 08540

Professor L. Sirovich
Division of Applied Mathematics
Brown University
Providence, RI 02912

Dr. P. K. Dai (RI/2178)
TRW Systems Group, Inc.
One Space Park
Redondo Beach, CA 90278

Redstone Scientific Information Center
Chief, Document Section
Army Missile Command
Redstone Arsenal, AL 35809

U.S. Army Research Office
P. O. Box 12211
Research Triangle, NC 27709

Editor, Applied Mechanics Review
Southwest Research Institute
8500 Culebra Road
San Antonio, TX 78228

Library and Information Services
General Dynamics-CONVAIR
P. O. Box 1128
San Diego, CA 92112

Dr. R. Magnus
General Dynamics-CONVAIR
Kearny Mesa Plant
P. O. Box 80847
San Diego, CA 92138

Mr. T. Brundage
Defense Advanced Research Projects
Agency
Research and Development Field Unit
APO 146, Box 271
San Francisco, CA 96246

Office of Naval Research
San Francisco Area Office
One Hallidie Plaza, Suite 601
San Francisco, CA 94102

Library
The RAND Corporation
1700 Main Street
Santa Monica, CA 90401

Dr. P. E. Rubbert
Boeing Aerospace Company
Boeing Military Airplane Development
Organization
P. O. Box 3707
Seattle, WA 98124

Dr. H. Yoshihara
Boeing Aerospace Company
P. O. Box3999
Mail Stop 41-18
Seattle, WA 98124

Mr. R. Feldhuhn
Naval Surface Weapons Center
White Oak Laboratory
Silver Spring, MD 20910

Librarian
Naval Surface Weapons Center
White Oak Laboratory
Silver Spring, MD 20910

Dr. J. M. Solomon
Naval Surface Weapons Center
White Oak Laboratory
Silver Spring, MD 20910

Professor J. H. Ferziger
Department of Mechanical Engineering
Stanford University
Stanford, CA 94305

Professor K. Karamcheti
Department of Aeronautics and
Astronautics
Stanford University
Stanford, CA 94305

Professor M. van Dyke
Department of Aeronautics and
Astronautics
Stanford University
Stanford, CA 94305

Professor O. Bunemann
Institute for Plasma Research
Stanford University
Stanford, CA 94305

Engineering Library
McDonnell Douglas Corporation
Department 218, Building 101
P. O. Box 516
St. Louis, MO 63166

Dr. R. J. Hakkinen
McDonnell Douglas Corporation
Department 222
P. O. Box 516
St. Louis, MO 63166

Dr. R. P. Heinisch
Honeywell, Inc.
Systems and Research Division -
Aerospace Defense Group
2345 Walnut Street
St. Paul, MN 55113

Dr. N. Malmuth
Rockwell International Science Center
1049 Camino Dos Rios
P. O. Box 1085
Thousand Oaks, CA 91360

Library
Institute of Aerospace Studies
University of Toronto
Toronto 5, Canada

Professor W. R. Sears
Aerospace and Mechanical Engineering
University of Arizona
Tucson, AZ 85721

Professor A. R. Seebass
Department of Aerospace and Mechanical
Engineering
University of Arizona
Tucson, AZ 85721

Dr. K. T. Yen
Code 3015
Naval Air Development Center
Warminster, PA 18974

Air Force Office of Scientific Research
(SREM)
Building 1410, Bolling AFB
Washington, DC 20332

Chief of Research and Development
Office of Chief of Staff
Department of the Army
Washington, DC 20310

Library of Congress
Science and Technology Division
Washington, DC 20540

Director of Research (Code RR)
National Aeronautics and Space
Administration
600 Independence Avenue, SW
Washington, DC 20546

Library
National Bureau of Standards
Washington, DC 20234

National Science Foundation
Engineering Division
1800 G Street, NW
Washington, DC 20550

Mr. W. Koven
AIR 03E
Naval Air Systems Command
Washington, DC 20361

Mr. R. Siewert
AIR 320D
Naval Air Systems Command
Washington, DC 20361

Technical Library Division
AIR 604
Naval Air Systems Command
Washington, DC 20361

Code 2627
Naval Research Laboratory
Washington, DC 20375

SEA 03512
Naval Sea Systems Command
Washington, DC 20362

SEA 09G3
Naval Sea Systems Command
Washington, DC 20362

Dr. A. L. Slafkosky
Scientific Advisor
Commandant of the Marine Corps
(Code AX)
Washington, DC 20380

Director
Weapons Systems Evaluation Group
Washington, DC 20305

Chief of Aerodynamics
AVCO Corporation
Missile Systems Division
201 Lowell Street
Wilmington, MA 01887

Research Library
AVCO Corporation
Missile Systems Division
201 Lowell Street
Wilmington, MA 01887

AFAPL (APRC)
AB
Wright Patterson, AFB, OH 45433

Dr. Donald J. Harney
AFFDL/FX
Wright Patterson AFB, OH 45433